Co-Design of Energy Storage and Resource Management for Cell-Free Radio Access Networks

Xiaojing Chen, Yijun Ding, Xiaomei Zhang, Wei Ni, *Fellow, IEEE*, Yichuang Sun, *Life Senior Member, IEEE*, Xin Wang, *Fellow, IEEE*, and Shunqing Zhang, *Senior Member, IEEE*

***Abstract*—Cell-free radio access network (CF-RAN) has emerged to address escalating demands in future mobile communications. The growing energy expense of CF-RAN necessitates efficient resource management and the integration of renewable energy harvesting systems. While prior studies on renewable energy-enabled CF-RAN have mainly focused on antenna resource management and energy consumption of access points (APs), they have largely overlooked significant power usage and scheduling requirements of central processing unit (CPU) and joint photovoltaic (PV) panel/battery sizing. To bridge these gaps, this paper integrates CF-RAN with smart grid technology and explores the joint optimization of PV panel/battery sizing and resource allocation to minimize system cost, including both capital expenditure (CAPEX) for PV/battery installation and operational expenditure (OPEX) for long-term operations. Leveraging the stochastic dual-subgradient method, we develop an online energy trading and resource allocation (OER) algorithm to enable real-time decisions on beamforming, service scheduling, and energy management. The feasibility and asymptotic optimality of the proposed OER are rigorously established through Lyapunov optimization techniques. Building on this asymptotically optimal solution, particle swarm optimization (PSO) is further employed to optimize the sizes of PV panels and batteries beforehand. Simulation results demonstrate a 62.7% reduction in total system cost compared to benchmark approaches, while reducing computational complexity in sizing PV panels and batteries.**

***Index Terms*—Cell-free radio access network (CF-RAN), photovoltaic (PV) panel and battery sizing, energy harvesting, resource allocation, stochastic optimization.**

I. Introduction

To meet the explosive demands of high data rates, multimedia applications and spectral efficiency for future mobile communications, e.g., sixth-generation (6G) system, cell-free radio access network (CF-RAN) has been proposed as a promising architecture with densely deployed access points (APs) connected to a central processing unit (CPU) via fronthaul links [2]–[4]. However, with the potentially substantially increased number of deployed APs and intensive processing needs at the CPU, the energy expenses contribute a significant part of the operational expenditure (OPEX).

Meanwhile, electricity grids are shifting from traditional grids to smart grids [5]. Smart grid technology enables flexible power schedules and two-way energy transactions in response to varying electricity prices, particularly with the integration of distributed renewable energy source (RES). It has the great potential to reduce the energy consumption and OPEX of wireless networks [6]–[9]. Several studies have investigated resource allocation to minimize the OPEX of smart grid-powered coordinated multipoint (CoMP) systems [10] or mobile edge computing (MEC) [11], [12]. While integrating RES, particularly photovoltaic (PV) systems, with CF-RAN is a natural strategy to curtail OPEX and carbon emissions, harnessing solar energy in wireless networks is far from straightforward. In contrast to reliable grid power, the output of PV panels is inherently intermittent, as it depends on solar insolation that varies with weather conditions, geographic location, and time of day [13]. Consequently, batteries are therefore essential to store surplus energy and stabilize supply. Yet, determining the optimal sizes of PV panels and batteries is an essential challenge: Oversizing leads to excessive capital expenditure (CAPEX) [14], [15], while undersizing increases reliance on grid electricity and raises OPEX. Crucially, these sizing decisions directly influence the efficiency of real-time resource allocation and energy trading strategies. Therefore, *to minimize the total system cost (including both CAPEX and OPEX) in smart grid-powered CF-RAN, PV panel/battery sizes must be carefully designed in conjunction with two-way energy transactions with the grid, battery charging/discharging schedules, and resource allocation.*

To address the computational complexity arising from the coupling of hardware sizing and stochastic resource management, we propose a two-stage framework, termed PBS-OER, which jointly integrates particle swarm optimization (PSO)-based sizing with online energy trading and resource allocation (OER) in smart grid-powered CF-RAN. Unlike the conference version [1] which adopted a cellular centralized C-RAN model, this work builds upon a CF-RAN architecture, where distributed APs jointly serve UEs without predefined cell boundaries. By jointly optimizing PV panel and battery sizing together with radio and energy resource allocation, the proposed PBS-OER minimizes system cost while ensuring system

This work was supported by the National Key R&D Program of China grants 2022YFB2902304 and 2022YFB2902303, and Shanghai Municipal Science and Technology Commission Foundation grants 25DP1500300 and 24DP1500703. A preliminary version of this work was presented at IEEE SPAWC 2023 [1]. *(Xiaojing Chen, Yijun Ding and Xiaomei Zhang contributed equally to this work.) (Corresponding author: Shunqing Zhang.)*

X. Chen, Y. Ding, X. Zhang, and S. Zhang are with the Key Laboratory of Specialty Fiber Optics and Optical Access Networks, Shanghai University, Shanghai 200444, China. X. Chen is also with the College of Computing and Data Science, Nanyang Technological University, Singapore 639798. Emails: {jodiechen, dingyijun, xiaomeizhang, shunqing}@shu.edu.cn.

W. Ni is with the School of Engineering, Edith Cowan University, Perth, WA 6027, and the School of Computer Science and Engineering, University of New South Wales, Sydney, NSW 2052, Australia. Email: wei.ni@ieee.org.

Y. Sun is with the Department of Engineering and Technology, University of Hertfordshire, Hatfield AL10 9AB, U.K. E-mail: y.sun@herts.ac.uk.

X. Wang is with the Key Laboratory for Information Science of Electromagnetic Waves (MoE), Department of Communication Science and Engineering, Fudan University, Shanghai 200433, China. E-mail: xwang11@fudan.edu.cn.

stability and users' QoS. PBS-OER consists of two tightly integrated stages. In the *offline stage*, a PSO-based algorithm determines the optimal PV panel and battery sizes for each AP using historical channel and energy price data, leveraging its efficiency in handling high-dimensional, non-convex search spaces without gradient information. In the *online stage*, the OER algorithm performs real-time beamforming, service scheduling and energy management based on the stochastic dual-subgradient method. Using Lyapunov optimization, OER is shown to achieve feasibility and asymptotic optimality, ensuring long-term system stability and QoS, which in turn enables efficient and high-quality sizing decisions.

The key contributions of this paper are summarized as follows:

1) We formulate the first joint PV panel/battery sizing and resource allocation problem tailored to CF-RAN. Unlike prior works on small cells or conventional RAN [16], [17], our formulation explicitly captures the coupling between hardware sizing, centralized beamforming, CPU computation scheduling, and energy trading. This holistic design minimizes both CAPEX and OPEX under smart grid integration.
2) We propose PBS-OER, a two-stage framework that co-designs offline PSO-based sizing with online energy trading and resource allocation. The framework incorporates CPU VM energy consumption and service scheduling into CF-RAN optimization. Leveraging the stochastic dual-subgradient method, real-time VM scheduling and energy management decisions for APs and CPUs are decoupled across time and entities, enabling fully distributed online optimization via OER.
3) Leveraging Lyapunov optimization, we establish the feasibility and asymptotic optimality of the proposed OER algorithm. Even when system dynamics such as RES generation and energy prices are unknown *a priori*, OER guarantees long-term stability and QoS.
4) With the asymptotically optimal OER in place, we employ PSO to efficiently determine PV panel and battery sizes in advance, utilizing historical system parameters (e.g., channel gains and energy prices).

Extensive simulations show that the proposed PBS-OER algorithm significantly cuts down the system cost by 62.7%, and reduces the computational complexity of the PV panel/battery sizing, compared to the benchmarks. The feasibility condition established analytically is also validated.

The remainder of the paper is organized as follows. In Section II, we review the related works. The system models are provided in Section III. In Section IV, the problem is formulated and relaxed to improve tractability. The proposed PBS-OER strategy is developed in Section V. Performance analysis is presented in Section VI. Numerical results are reported in Section VII, while Section VIII provides conclusions. The notation used in this paper is listed in Table II.

II. Related Work

Some works have investigated resource allocation for RES-enabled CF-RAN [18]–[20], and its predecessor C-RAN [21], [22]. Demir *et al.* [18] applied linear programming for offline energy cooperation and management of cell-free massive multiple-input multiple-output (CF-mMIMO) systems. Moradi *et al.* [19] developed an AP power allocation scheme to minimize the energy consumption from the electrical grid. An intelligent network resource scheduling scheme based on the Soft Actor-Critic (SAC) algorithm was proposed in [20] to provide quality-of-service (QoS) guarantees while minimizing grid power consumption. Focusing on practical random systems, online resource management schemes were studied based on Lyapunov optimization in [21] with RES-powered APs. Zeng *et al.* [22] investigated an RES-aware AP activation problem with convex optimization to verify the high energy efficiency of their green C-RAN architecture. Despite these contributions, the existing works [18]–[22] primarily focus on antenna resource management and the energy consumption of APs. They largely overlook the substantial power usage and scheduling requirements of CPU virtual machines (VMs). Moreover, none of these studies jointly optimize PV panel/battery sizing together with radio and energy resource allocation in CF-RAN.

In parallel, several studies have examined PV panel and battery sizing in cellular networks. Chamola *et al.* [23] analyzed the outage probability with regard to PV panel size and battery number by modeling solar energy harvesting, BS load, and battery state as Markov processes. Javidsharifi *et al.* [14] developed a heuristic algorithm to decide the number of PV panels and battery capacities for powering drone-aided cellular networks. Only a few existing works have jointly considered PV panel/battery sizing and radio/energy resource allocation, for smart grid-powered small cells [16] or RES-enabled RAN [17]. Mendil *et al.* [16] developed an iterative approach for PV panel/battery sizing accounting for battery aging, and minimized energy cost using a Fuzzy Q-learning based energy control strategy. Pamuklu *et al.* [17] proposed an offline cost-effective algorithm for PV panel/battery sizing, and an online BS switch-on/off algorithm to regulate the grid electricity consumption. Although these works represent important steps towards green wireless networks, their approaches are tailored to decentralized small-cell or conventional RAN architectures and cannot be directly extended to CF-RAN, which involves complex centralized beamforming and joint signal processing across all APs. Furthermore, none of them provides an online stochastic optimization framework with rigorous theoretical guarantees that can simultaneously handle renewable energy intermittency and dynamic energy prices.

Table I provides a structured comparison of the above related works and the proposed approach. As summarized in the table, three open problems motivate this work:

1) *Oversight of CPU computation resources*: Prior works on RES-enabled CF-RAN or C-RAN [18]–[22] mainly focus on antenna resource management and energy consumption of APs, and overlook the significant power usage and scheduling requirements of CPU VMs.
2) *Absence of joint optimization in CF-RAN*: While a few works on small cells and conventional RAN [16], [17] have investigated joint PV panel/battery sizing and resource allocation, their approaches cannot be directly

TABLE I
SUMMARY OF RELATED WORKS AND CRITICAL GAPS

Reference	System	Architecture	Objective	Main Focus	Gap
Demir *et al.* [18]	RES-enabled CF-RAN	Distributed APs; centralized CPU	Spectral efficiency	Offline energy cooperation via linear programming	✓AP energy consumption and antenna resource management; ✗CPU computation resource scheduling; ✗PV/battery sizing; ✗online optimization with theoretical guarantees.
Moradi *et al.* [19]	RES-enabled CF-RAN	Distributed APs; centralized CPU	Energy consumption	AP power allocation to minimize energy consumption	
Zhang *et al.* [20]	RES-enabled CF-RAN	Distributed APs; centralized CPU	Energy consumption	SAC-based intelligent scheduling for QoS and grid power minimization	
Zhu *et al.* [21]	RES-enabled C-RAN	Centralized	Energy efficiency	Online resource management via Lyapunov optimization	
Zeng *et al.* [22]	RES-enabled C-RAN	Centralized	Energy consumption	RES-aware AP activation with convex optimization	
Chamola *et al.* [23]	RES-enabled cellular networks	Decentralized	CAPEX	Outage analysis with PV/battery sizing (Markov modeling)	✓PV/battery sizing; ✗joint radio and energy resource allocation; ✗CF-RAN specific.
Javidsharifi *et al.* [14]	Drone-aided cellular networks	Decentralized	OPEX+ CAPEX	Heuristic PV/battery sizing algorithm	
Mendil *et al.* [16]	Smart grid-powered small cells	Decentralized	OPEX+ CAPEX	Iterative PV/battery sizing with battery aging; fuzzy Q-learning	✓Joint PV/battery sizing and resource allocation; ✗directly extended to CF-RAN; ✗CF-RAN-oriented online stochastic optimization.
Pamuklu *et al.* [17]	RES-enabled RAN	Decentralized	OPEX+ CAPEX	Offline PV/battery sizing; online BS switch-on/off	
Proposed PBS-OER	**Smart grid-powered CF-RAN**	**Distributed APs; centralized CPU**	**OPEX+ CAPEX**	**Joint PV/battery sizing and online resource allocation**	**✓CPU resource scheduling; ✓joint PV/battery sizing and resource allocation for CF-RAN; ✓online stochastic optimization with theoretical guarantees.**

extended to CF-RAN. The CF-RAN architecture requires complex beamforming and centralized processing, which creates a unique coupling between hardware sizing and real-time signal processing that has not been studied in the literature.

3) *Lack of CF-RAN-oriented online stochastic optimization with theoretical guarantees*: Existing methods do not provide an online optimization framework with theoretical guarantees that can simultaneously handle renewable energy intermittency and dynamic energy prices in CF-RAN, making it difficult to ensure long-term stability and QoS.

As clearly highlighted in Table I, the proposed PBS-OER is the only approach that simultaneously addresses CPU computation resources, joint PV/battery sizing and resource allocation tailored to CF-RAN, and online stochastic optimization with theoretical guarantees.

III. SYSTEM MODELS

Consider a CF-RAN for downlink transmission; see Fig. 1. A set $\mathcal{I} := \{1, \ldots, I\}$ of multi-antenna APs, each equipped with M antennas, serves a set $\mathcal{K} := \{1, \ldots, K\}$ of single-antenna user equipment (UE). All APs are linked to the CPU through highly reliable wired fronthaul links (e.g., optical fibers). The CPU builds VMs to provide computational resources to the UEs. Suppose that the CPU and each AP can use batteries to store surplus RES harvested by the PV panels and electricity purchased off the grid for their future use.

We consider slotted transmissions and model the wireless channels and RES harvesting process as quasi-static models; i.e., the channel coefficients and harvested energy amounts do not change within a time slot, and yet can change independently between slots. Let $t \in \mathcal{T} := \{0, 1, 2, \ldots, T-1\}$ denote the index of a slot. The duration of a slot is normalized to "1" for illustration convenience. In this sense, the terms "energy" and "power" are interchangeable in this paper.

TABLE II
NOTATION AND DEFINITION

Notation	Definition
$\mathcal{I}, I$	Set and total number of APs
$\mathcal{K}, K$	Set and total number of UEs
M	Number of antennas per AP
T, t	Operation period and time slot index
$C_{\text{pv}}, C_{\text{bat}}$	Unit costs for PV panels and batteries
$\mathbf{h}_{ik}^t, \mathbf{w}_{ik}^t$	Channel gain and beamforming vectors from AP i to UE k
$r_k^t, \gamma_k, n_k^t, \sigma_k^2$	Transmission rate, target SINR, noise and noise variance of UE k
$Q_{e,k}^t, Q_{u,k}^t$	Queue lengths of VM processing at CPU and transmission at APs for UE k
A_k^t, λ_k	Data arrival amount and average arrival rate for UE k at the CPU
$\mu_k^t, \mu_k^{\max}$	Service rate and maximum service rate of VM k at the CPU
E_i^t, E_e^t	Harvested RES at AP i and CPU
S_i, I_i^t	PV panel size and solar insolation at AP i
C_i^t, C_e^t	State of Charge (SoC) of battery at AP i and CPU
$C_i^{\max}, C_e^{\max}$	Battery capacity at AP i and CPU
$C_i^{\min}, C_e^{\min}$	Minimum battery energy level at AP i and CPU
$P_{b,i}^t, P_{b,e}^t$	Battery charging/discharging power at AP i and CPU
$P_{g,i}^t, P_{c,i}$	Total power consumption and constant power consumption of AP i
$P_{v,e}^t, P_{\text{coord}}$	Total power consumption and constant coordination power of the CPU
α^t, β^t	Effective energy buying and selling prices at slot t
$\Phi_{\text{CAP}}, \Phi_{\text{OP}}$	CAPEX and OPEX
$G_R(\cdot), G_B(\cdot)$	Transaction cost of APs and CPU
q_i^t, q_e^t	Virtual energy queues of AP i and CPU

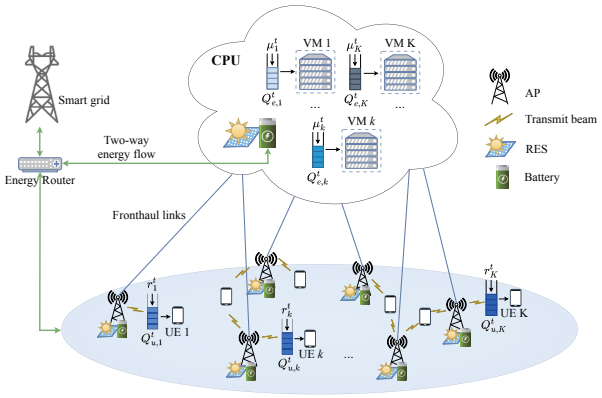

Fig. 1. The considered smart grid-powered CF-RAN, where the CPU and APs with a mixed power supply implement two-way energy transactions with the smart grid.

As per slot t, $\mathbf{h}_{ik}^t \in \mathbb{C}^M$ is the channel gain from AP i to UE k, and $\mathbf{w}_{ik}^t \in \mathbb{C}^M$ is the beamformer of AP i to UE k. The channel gain and beamforming vector from the APs to UE k are collected in $\mathbf{h}_k^t := [\mathbf{h}_{1k}^{t'}, \ldots, \mathbf{h}_{Ik}^{t'}]' \in \mathbb{C}^{MI}$ and $\mathbf{w}_k^t := [\mathbf{w}_{1k}^{t'}, \ldots, \mathbf{w}_{Ik}^{t'}]' \in \mathbb{C}^{MI}$. The received signal at UE k is [3], [18]

$$y_k^t = \mathbf{h}_k^{t^H} \mathbf{w}_k^t x_k^t + \sum_{j=1, j\neq k}^{K} \mathbf{h}_k^{t^H} \mathbf{w}_j^t x_j^t + n_k^t, \tag{1}$$

where x_k^t is the normalized data symbol for UE k with unit power; n_k^t is the additive noise at UE k, following the circularly symmetric complex Gaussian distribution with zero mean and variance σ_k^2. The first term on the right-hand side (RHS) of (1) accounts for the desired coherent signal jointly transmitted from all APs serving UE k. The second term corresponds to coherent multi-user signals intended for other UEs, which are jointly processed in CF-RAN. The signal-to-interference-plus-noise-ratio (SINR) of UE k is given by [3]

$$\text{SINR}_k^t(\{\mathbf{w}_k^t\}) = \frac{\mathbf{h}_k^{t^H} \mathbf{w}_k^t \mathbf{w}_k^{t^H} \mathbf{h}_k^t}{\sum_{j=1, j\neq k}^{K} \mathbf{h}_k^{t^H} \mathbf{w}_j^t \mathbf{w}_j^{t^H} \mathbf{h}_k^t + \sigma_k^2}. \tag{2}$$

With γ_k denoting UE k's target SINR, the QoS of UEs is guaranteed by requiring [18]

$$\text{SINR}_k^t(\{\mathbf{w}_k^t\}) \geq \gamma_k, \quad \forall k. \tag{3}$$

The achievable rate of UE k at slot t is

$$r_k^t(\{\mathbf{w}_k^t\}) = \log(1 + \frac{\mathbf{h}_k^{t^H} \mathbf{w}_k^t \mathbf{w}_k^{t^H} \mathbf{h}_k^t}{\sum_{j=1, j\neq k}^{K} \mathbf{h}_k^{t^H} \mathbf{w}_j^t \mathbf{w}_j^{t^H} \mathbf{h}_k^t + \sigma_k^2}). \tag{4}$$

A. Queue Model

A double-layer queueing model is created to describe data processing and transmission from the CPU to the UEs with reference to [24]. Assume that each UE k is exclusively served by its respective VM k. As shown in Fig. 1, the data of UE k arrives at the processing queue of VM k in the CPU, and is executed with a service rate of $\mu_k^t \in [0, \mu_k^{\max}]$, where $\mu_k^{\max}$ denotes the maximum service rate. The service rate inherently captures the non-negligible processing delay at the CPU. The processed data is delivered to the transmission queue of the AP serving UE k, and then to UE k via wireless channels with the transmit rate r_k^t in (4).

Let $Q_{e,k}^t$ and $Q_{u,k}^t$ denote the lengths of the VM processing queue and AP transmission queue for UE k at slot t, respectively. With $[x]^+ := \max\{x, 0\}$, these two queues evolve as

$$Q_{e,k}^{t+1} = [Q_{e,k}^t - \mu_k^t]^+ + A_k^t; \quad Q_{u,k}^{t+1} = [Q_{u,k}^t - r_k^t]^+ + \mu_k^t, \tag{5}$$

where A_k^t denotes the data for UE k arriving at the CPU at slot t with an average arrival rate of $\lambda_k = \mathbb{E}\{A_k^t\}$. Note that the service rate μ_k^t not only determines the execution speed at VM k but also represents the data rate forwarded from the CPU to the AP serving UE k. Each fronthaul link between an AP i and the CPU is subject to a finite capacity $C_{\text{fh},i}$. To capture fronthaul limitations, we impose

$$\mu_k^t \leq w_{k,i} C_{\text{fh},i}, \ \sum_{k\in\Gamma_i} w_{k,i} = 1, \tag{6}$$

where $w_{k,i}$ is the allocation weight (e.g., based on channel quality or service priority), and Γ_i denotes the set of UEs served by AP i.

We define the system as stable if the following holds:

$$\lim_{T\to\infty} \frac{1}{T} \sum_{t=0}^{T-1} \mathbb{E}[Q_{e,k}^t] \leq \infty; \quad \lim_{T\to\infty} \frac{1}{T} \sum_{t=0}^{T-1} \mathbb{E}[Q_{u,k}^t] \leq \infty. \tag{7}$$

B. Energy Model

1) Energy Consumption: The transmit power of AP i is $P_{x,i}^t = \sum_{k=1}^{K} \mathbf{w}_k^{t^H} \mathbf{B}_i \mathbf{w}_k^t$, where the $MI \times MI$ matrix $\mathbf{B}_i := \text{diag}(\underbrace{0, \ldots, 0}_{(i-1)M}, \underbrace{1, \ldots, 1}_{M}, \underbrace{0, \ldots, 0}_{(I-i)M})$ selects the beamforming vectors $\mathbf{w}_{i,k}^t, \forall i$ from $\mathbf{w}_k^t$, for evaluating the transmit power of AP i. The total power consumption of AP i at slot t is

$$P_{g,i}^t = P_{c,i} + \sum_{k=1}^{K} \mathbf{w}_k^{t^H} \mathbf{B}_i \mathbf{w}_k^t / \xi \leq P_{g,i}^{\max}, \tag{8}$$

where $P_{c,i}$ is the constant power consumed by, e.g., air conditioning, data processing and circuits; $\xi > 0$ specifies the power amplifier efficiency; $P_{g,i}^{\max}$ is the maximum power consumption of AP i. By default, we set $\xi = 1$.

The power consumption for user data processing of a VM is generally considered as a convex and increasing function of the service rate μ_k^t [25], [26]. To account for the additional computational burden of centralized scheduling and coordination, the CPU power consumption is given by $P_{v,e}^t = \sum_{k=1}^{K} k_c (\mu_k^t)^3 + P_{\text{coord}}$, where the first term on the RHS represents the processing cost for user data, and P_{coord} explicitly models the overhead of joint coordination. Here, $k_c > 0$ is a constant, and typically obtained empirically.

2) Renewable Energy Generation: Suppose that the sizes of the PV panel and battery at the CPU are known, while those at the APs can be optimized to reduce the system cost. The RES harvested at the CPU at slot t is E_e^t. The RES harvested at AP i at slot t is $E_i^t = \eta_{pv} \cdot S_i \cdot I_i^t$, where I_i^t denotes the solar insolation of AP i, S_i is the size (or area) of the PV panel, and η_{pv} is the PV module efficiency [27], [28]. Note that renewable generation (e.g., solar insolation I_i^t) is modeled as a random

process rather than a deterministic input, thereby capturing environmental uncertainties. Without loss of generality, we set $\eta_{pv} = 1$ by default.

3) Battery Dynamics: Considering physical constraints, each battery has a finite capacity and a minimum energy level for the battery's health. The state of charge (SoC) of the APs, denoted by C_i^t, and of the CPU, denoted by C_e^t, the battery (dis)charge rates at the APs, $P_{b,i}^t$, and at the CPU, $P_{b,e}^t$, satisfy

$$C_i^{t+1} = C_i^t + P_{b,i}^t,\ C_i^{\min} \le C_i^t \le C_i^{\max},\ \forall i, t \tag{9}$$

$$C_e^{t+1} = C_e^t + P_{b,e}^t,\ C_e^{\min} \le C_e^t \le C_e^{\max},\ \forall t \tag{10}$$

$$P_{b,i}^{\min} \le P_{b,i}^t \le P_{b,i}^{\max},\ P_{b,e}^{\min} \le P_{b,e}^t \le P_{b,e}^{\max},\ \forall t \tag{11}$$

where $P_{b,i}^{\min} < 0$ and $P_{b,e}^{\min} < 0$ are the maximum battery discharging amounts, and $P_{b,i}^{\max} > 0$ and $P_{b,e}^{\max} > 0$ are the maximum battery charging amounts accordingly.

4) Energy Trading Mechanism: Given the batteries, two-way energy transactions between the CPU/APs and the grid can better utilize the RES and cut down system cost. The energy shortage of the CPU to be acquired from the grid is $[P_{v,e}^t - E_e^t + P_{b,e}^t]^+$. The surplus energy that can be sold to the grid is $[E_e^t - P_{v,e}^t - P_{b,e}^t]^+$. The shortage energy of AP i is $[P_{g,i}^t - S_i I_i^t + P_{b,i}^t]^+$. Its surplus energy is $[S_i I_i^t - P_{g,i}^t - P_{b,i}^t]^+$.

Let $\tilde{\alpha}^t$ and $\tilde{\beta}^t$ be the energy purchase and selling prices at time t, respectively. It is reasonable to assume $\tilde{\alpha}^t > \tilde{\beta}^t > 0$. To capture battery (dis)charging inefficiencies, we pre-scale $\tilde{\alpha}^t$ and $\tilde{\beta}^t$ to obtain effective energy prices: $\alpha^t = \tilde{\alpha}^t/\eta_{\text{ch}}$ and $\beta^t = \tilde{\beta}^t \eta_{\text{dis}}$, where η_{ch} and η_{dis} are the battery charging and discharging efficiencies, respectively. The transaction cost of the CPU at time t is given by

$$G_B(P_{v,e}^t, P_{b,e}^t) := \alpha^t [P_{v,e}^t - E_e^t + P_{b,e}^t]^+ - \beta^t [E_e^t - P_{v,e}^t - P_{b,e}^t]^+. \tag{12}$$

The transaction cost of AP i at slot t is

$$\begin{aligned} G_R(S_i, P_{g,i}^t, P_{b,i}^t) := {} & \alpha^t [P_{g,i}^t - S_i I_i^t + P_{b,i}^t]^+ \\ & - \beta^t [S_i I_i^t - P_{g,i}^t - P_{b,i}^t]^+. \end{aligned} \tag{13}$$

The system OPEX is considered as the total energy transaction cost over a long-term horizon T, i.e.,

$$\Phi_{\text{OP}}(S_i, P_i^t, P_e^t) = \sum_{t=0}^{T-1} [\sum_{i \in \mathcal{I}} G_R(S_i, P_i^t) + G_B(P_e^t)],$$

where $P_i^t := P_{g,i}^t + P_{b,i}^t$ and $P_e^t := P_{v,e}^t + P_{b,e}^t$ are auxiliary variables introduced for notational brevity.

The system CAPEX can be modeled as a linear function of the sizes of PV panels and batteries at the APs [17], as given by

$$\Phi_{\text{CAP}}(S_i, C_i^{\max}) = \sum_{i \in \mathcal{I}} (S_i \cdot C_{\text{pv}} + C_i^{\max} \cdot C_{\text{bat}}), \tag{14}$$

where C_{pv} is the unit installation cost of a PV panel. Considering the effect of battery degradation, we amortize the expected replacement cost over the planning horizon T and embed it into the CAPEX coefficient. Specifically, we define the effective unit cost of battery as $C_{\text{bat}} = C_{\text{bat}}^{\text{ins}} + C_{\text{bat}}^{\text{rep}}$, where $C_{\text{bat}}^{\text{ins}}$ is the unit installation cost, and $C_{\text{bat}}^{\text{rep}}$ is the amortized unit replacement cost given by $C_{\text{bat}}^{\text{rep}} = c_{\text{rep}} \eta_{\text{cyc}} T / L_{\text{nom}}$ [29], [30]. Here, c_{rep} denotes the replacement cost per unit capacity, η_{cyc} is the cycle-induced capacity loss coefficient, and L_{nom} denotes the nominal cycle lifetime of the battery.

IV. Problem Formulation

In this section, we investigate the PV panel/battery sizing and radio/energy resource allocation for the smart grid-powered CF-RAN to minimize the system cost (including CAPEX and long-term OPEX), while guaranteeing the system stability and UEs' QoS requirement. The problem is cast as

$$\textbf{P1:}\ \min_{\Theta}\ \Phi_{\text{CAP}}(S_i, C_i^{\max}) + \Phi_{\text{OP}}(S_i, P_i^t, P_e^t) \tag{15a}$$

$$\text{s. t.}\ \ S_i^{\min} \le S_i \le S_i^{\max},\ C_i^{\text{MIN}} \le C_i^{\max} \le C_i^{\text{MAX}}, \tag{15b}$$

$$C_i^{\min} \le C_i^t \le C_i^{\max},\ C_e^{\min} \le C_e^t \le C_e^{\max}, \tag{15c}$$

$$C_i^{t+1} = C_i^t + P_i^t - P_{c,i} - \sum_{k \in \mathcal{K}} \mathbf{w}_k^{t\,H} \mathbf{B}_i \mathbf{w}_k^t, \tag{15d}$$

$$C_e^{t+1} = C_e^t + P_e^t - k_{\text{c}} \sum_{k \in \mathcal{K}} (\mu_k^t)^3, \tag{15e}$$

$$(3),\ (5) - (8),\ (11),$$

where $\Theta := \{S_i, C_i^{\max}, \mathbf{w}_k^t, \mu_k^t, P_i^t, P_e^t, \forall i, k, t\}$. Here, S_i and $C_i^{\max}$ are bounded in (15b), and are assumed to be discrete values picked from finite sets.

Problem **P1** is nontrivial, as the PV panel and battery sizing decisions made in advance affect the real-time resource allocation and energy trading over the long-time operation period. Moreover, the SoC dynamics in (15d)–(15e) and the queue changes in (5) couple all variables $\{\mathbf{w}_k^t, \mu_k^t, P_i^t, P_e^t, \forall i, k, t\}$ throughout T. We proceed to decompose Problem **P1** into two subproblems: a long-term time-average OPEX minimization subproblem with fixed PV panel and battery sizes, and a one-off PV panel/battery sizing subproblem that minimizes the total system cost, and produce an asymptotically optimal solution, as will be discussed in Section V.

1) OPEX Minimization: Let $\boldsymbol{x}^t := \{\mathbf{w}_k^t, \mu_k^t, P_i^t, P_e^t, \forall i, k\}$, and $\mathcal{X} := \{\boldsymbol{x}^t, \forall t\}$. Given the PV panel sizes and batteries, the long-term time-average OPEX minimization is cast as

$$\textbf{S1:}\ F^* := \min_{\mathcal{X}} \lim_{T \to \infty} \frac{1}{T} \sum_{t=0}^{T-1} [\sum_{i \in \mathcal{I}} G_R(P_i^t) + G_B(P_e^t)] \tag{16}$$

$$\text{s. t.}\ \ (3),\ (5)\text{–}(8),\ (11),\ (15c)\text{–}(15e).$$

2) PV Panel and Battery Sizing: Based on the solution to Problem **S1**, the minimum OPEX F^* can be obtained with different size combinations of PV panels and batteries. Then the PV panel and battery sizing can be optimized by solving

$$\textbf{S2:}\ \min_{\{S_i, C_i^{\max}\}}\ \Phi_{\text{CAP}}(S_i, C_i^{\max}) + T F^*(S_i, C_i^{\max}) \tag{17}$$

$$\text{s. t.}\ \ (15b).$$

It is difficult to solve Problem **S1** since our goal is to minimize the time-average OPEX cost over a long time horizon, with all variables $\{\mathbf{w}_k^t, \mu_k^t, P_i^t, P_e^t, \forall i, k, t\}$ coupled in (5) and (15d)–(15e) throughout the operation period T.

We relax the problem to improve its tractability by applying time decoupling [31]. In particular, for the coupled battery

dynamics (15d)–(15e), as we sum them up over the scheduling horizon, and then divide both sides by $T \to \infty$, it holds that

$$\lim_{T\to\infty} \frac{1}{T} \sum_{t=0}^{T-1} \mathbb{E}[P_i^t - P_{c,i} - \sum_k \mathbf{w}_k^{tH} \mathbf{B}_i \mathbf{w}_k^t] = 0; \\ \lim_{T\to\infty} \frac{1}{T} \sum_{t=0}^{T-1} \mathbb{E}[P_e^t - k_c \sum_k (\mu_k^t)^3] = 0. \tag{18}$$

By reformulating (5) and (7) from a long-term perspective, the following conditions must be satisfied for system stability [32]

$$\lim_{T\to\infty} \frac{1}{T} \sum_{t=0}^{T-1} \mathbb{E}[A_k^t - \mu_k^t] \le 0; \\ \lim_{T\to\infty} \frac{1}{T} \sum_{t=0}^{T-1} \mathbb{E}[\mu_k^t - r_k^t] \le 0. \tag{19}$$

Problem **S1** can now be relaxed to

$$\textbf{S1.1:} \quad \widetilde{F}^* := \min_{\mathcal{X}} \mathbb{E}[\sum_{i\in\mathcal{I}} G_R(P_i^t) + G_B(P_e^t)] \\ \text{s. t. (3), (8), (11), (18)–(19).}$$

In Problem **S1.1**, (15c)–(15e) are replaced by (18) to eliminate the time coupling of $\{C_i^t, C_e^t, \forall i, t\}$. (5) and (7) are replaced by (19) to eliminate the time coupling of $\{Q_{e,k}^t, Q_{u,k}^t, \forall k, t\}$. Since Problem **S1.1** is a relaxed version of **S1**, a lower bound of F^* can be obtained by solving Problem **S1.1**. This is because the optimal value of **S1.1** does not exceed that of **S1**, i.e., $\widetilde{F}^* \le F^*$. Let $\boldsymbol{\xi}^t := \{I_i^t, E_e^t, A_k^t, \mathbf{h}_k^t, \alpha^t, \beta^t\}$ collect all the dynamic system parameters. We apply a stochastic dual-subgradient approach to solve Problem **S1.1**, so that the asymptotically optimal solution to **S1** can be obtained.

V. Proposed PBS-OER Algorithm

A. Online Resource Allocation

We develop an iterative algorithm to achieve a long-term optimal resource scheduling strategy (including AP beamforming, CPU processing, and energy transaction control) for **S1.1**.

1) Stochastic Dual-Subgradient Method: Let $\mathcal{F}^t$ denote the set of $\boldsymbol{x}^t$ satisfying constraints (3), (8) and (11) per t. Also, let $\boldsymbol{\lambda}^t := \{\lambda_{i,1}^t, \lambda_2^t, \lambda_{k,3}^t, \lambda_{k,4}^t, \forall i, k\}$ and $\boldsymbol{\lambda} := \{\boldsymbol{\lambda}^t, \forall t\}$ collect the Lagrange multipliers related with constraints (18) and (19). The partial Lagrangian function of Problem **S1.1** is given by $L(\mathcal{X}, \boldsymbol{\lambda}) := \mathbb{E}[L^t(\boldsymbol{x}^t, \boldsymbol{\lambda}^t)]$, where $L^t(\boldsymbol{x}^t, \boldsymbol{\lambda}^t)$ is the instantaneous Lagrangian at slot t, as given by

$$L^t(\boldsymbol{x}^t, \boldsymbol{\lambda}^t) = \sum_{i\in\mathcal{I}} G_R(P_i^t) + G_B(P_e^t) + \sum_{i\in\mathcal{I}} \lambda_{i,1}^t (P_i^t - P_{c,i} \\ - \sum_k \mathbf{w}_k^{tH} \mathbf{B}_i \mathbf{w}_k^t) + \lambda_2^t (P_e^t - k_c \sum_k (\mu_k^t)^3) \\ + \sum_{k\in\mathcal{K}} \lambda_{k,3}^t (A_k^t - \mu_k^t) + \sum_{k\in\mathcal{K}} \lambda_{k,4}^t (\mu_k^t - r_k^t(\{\mathbf{w}_k^t\})). \tag{21}$$

The dual problem of Problem **S1.1** is $\max_{\boldsymbol{\lambda}} D(\boldsymbol{\lambda})$, where $D(\boldsymbol{\lambda}) = \min_{\boldsymbol{x}^t\in\mathcal{F}^t} L(\mathcal{X}, \boldsymbol{\lambda})$. A standard subgradient method can be adopted to update $\boldsymbol{\lambda}$ for the dual problem. However, calculating the standard subgradients requires taking expectations over the random parameter $\boldsymbol{\xi}^t$ with unknown joint probability distributions. For a stationary $\boldsymbol{\xi}^t$, we apply the stochastic subgradient descent technique to update the stochastic Lagrange multipliers $\hat{\boldsymbol{\lambda}}^t = \{\hat{\lambda}_{i,1}^t, \hat{\lambda}_2^t, \hat{\lambda}_{k,3}^t, \hat{\lambda}_{k,4}^t, \forall i, k, t\}$ with the stepsize η, as given by [33]

$$\hat{\lambda}_{i,1}^{t+1} = \hat{\lambda}_{i,1}^t + \eta(P_i^t - P_{c,i} - \sum_k \mathbf{w}_k^{tH} \mathbf{B}_i \mathbf{w}_k^t), \ \forall i, t; \tag{22a}$$

$$\hat{\lambda}_2^{t+1} = \hat{\lambda}_2^t + \eta(P_e^t - k_c \sum_k (\mu_k^t)^3), \ \forall t; \tag{22b}$$

$$\hat{\lambda}_{k,3}^{t+1} = [\hat{\lambda}_{k,3}^t + \eta(A_k^t - \mu_k^t)]^+, \ \forall k, t; \tag{22c}$$

$$\hat{\lambda}_{k,4}^{t+1} = [\hat{\lambda}_{k,4}^t + \eta(\mu_k^t - r_k^t(\{\mathbf{w}_k^t\}))]^+, \ \forall k, t. \tag{22d}$$

With $\hat{\boldsymbol{\lambda}}^t$ obtained from $\boldsymbol{x}^{t-1}$ via (22) per t, we can optimize online the variables $\boldsymbol{x}^t = \{\mathbf{w}_k^t, \mu_k^t, P_i^t, P_e^t\}$ by solving

$$\boldsymbol{x}^t = \arg\min_{\boldsymbol{x}^t\in\mathcal{F}^t} L^t(\boldsymbol{x}^t, \hat{\boldsymbol{\lambda}}^t, \boldsymbol{\xi}^t). \tag{23}$$

2) Virtual-Queue Control: The queues of the VMs and UEs in (5) satisfy $Q_{e,k}^t = \hat{\lambda}_{k,3}^t/\eta$ and $Q_{u,k}^t = \hat{\lambda}_{k,4}^t/\eta$; see (22c) and (22d). Define two virtual energy queues $q_i^t = \hat{\lambda}_{i,1}^t/\eta$ and $q_e^t = \hat{\lambda}_2^t/\eta$, following the SoC dynamics (15d) and (15e), i.e.,

$$q_i^{t+1} = q_i^t + P_i^t - P_{c,i} - \sum_k \mathbf{w}_k^{tH} \mathbf{B}_i \mathbf{w}_k^t; \tag{24a}$$

$$q_e^{t+1} = q_e^t + P_e^t - k_c \sum_k (\mu_k^t)^3. \tag{24b}$$

The values of q_i^t and q_e^t are allowed to be negative.

3) Online Optimization: Let $\boldsymbol{Q}^t := \{q_i^t, q_e^t, Q_{e,k}^t, Q_{u,k}^t\}$, then $\hat{\boldsymbol{\lambda}}^t = \eta \boldsymbol{Q}^t$. We can replace $\hat{\boldsymbol{\lambda}}^t$ with $\eta \boldsymbol{Q}^t$ in (23), and decompose (23) into four subproblems based on the decision variables, i.e.,

$$\min_{P_i^t} f_1(P_i^t) = \min_{P_i^t} \sum_i [G_R(P_i^t) + \eta q_i^t (P_i^t - P_{c,i})], \\ \text{s. t. (11);} \tag{25a}$$

$$\min_{P_e^t} f_2(P_e^t) = \min_{P_e^t} [G_B(P_e^t) + \eta q_e^t P_e^t], \\ \text{s. t. (11);} \tag{25b}$$

$$\min_{\mu_k^t} f_3(\mu_k^t) = \min_{\mu_k^t} \sum_k [-\eta q_e^t k_c (\mu_k^t)^3 + \eta Q_{e,k}^t (A_k^t - \mu_k^t) \\ + \eta Q_{u,k}^t \mu_k^t], \\ \text{s. t. (11);} \tag{25c}$$

$$\min_{\mathbf{w}_k^t} f_4(\mathbf{w}_k^t) = \min_{\mathbf{w}_k^t} [-\sum_i \eta q_i^t \sum_k \mathbf{w}_k^{tH} \mathbf{B}_i \mathbf{w}_k^t - \sum_k \eta Q_{u,k}^t r_k^t(\{\mathbf{w}_k^t\})], \\ \text{s. t. (3), (8), (11).} \tag{25d}$$

In what follows, given $\boldsymbol{Q}^t$, we optimize energy management via (25a)-(25b), VM processing via (25c), and AP beamforming via (25d). The energy management (25a)-(25b) and VM service schedule (25c) problems are inherently distributed across APs/VMs, where local decision-making is performed. The beamforming design is coordinated centrally at the CPU.

- **Energy Management:** By defining $\psi^t := (\alpha^t - \beta^t)/2$ and $\phi^t := (\alpha^t + \beta^t)/2$, (12) and (13) can be rewritten as

$$G_B(P_e^t) = \psi^t \left| P_e^t - E_e^t \right| + \phi^t (P_e^t - E_e^t), \\ G_R(P_i^t) = \psi^t \left| P_i^t - S_i I_i^t \right| + \phi^t (P_i^t - S_i I_i^t).$$

Since $\alpha^t > \beta^t > 0$, it readily follows that $\phi^t > \psi^t > 0$. $G_B(P_e^t)$ and $G_R(P_i^t)$ are convex functions of P_e^t and P_i^t, respectively. As a result, (25a) and (25b) are convex of P_i^t and P_e^t, respectively, which can be solved by convex solvers, e.g., the interior-point method [34].

- **VM Service Schedule:** Subproblem (25c) minimizes a cubic function of μ_k^t. The optimal processing rate $\mu_k^{t,opt}$ can be obtained by setting $f_3^{'}(\mu_k^t) = 0$, where $f_3^{'}(\cdot)$ is the first-order derivative of $f_3(\cdot)$. We then have

$$\mu_k^{t,opt} = \begin{cases} \min[\sqrt{\frac{Q_{u,k}^t - Q_{e,k}^t}{3q_e^t k_c}}, \mu_k^{\max}], \text{ if } \frac{Q_{u,k}^t - Q_{e,k}^t}{q_e^t} > 0; \\ \mu_k^{\max}, \qquad\qquad \text{otherwise.} \end{cases} \tag{27}$$

- **AP Beamforming:** Subproblem (25d) is equivalent to the following weighted minimum mean square error (WMMSE) problem [35]:

$$\min_{\{\rho_k^t, u_k^t, \mathbf{w}_k^t\}} \sum_k \eta Q_{u,k}^t (\rho_k^t e_k^t - \log \rho_k^t) - \sum_i [\eta q_i^t \sum_k \mathbf{w}_k^{t^H} \mathbf{B}_i \mathbf{w}_k^t]. \tag{28}$$

This is because (25d) is equivalent to the weighted sum-rate (WSR) maximization, and the equivalence between WSR maximization and WMMSE problem has been established in [35]. Here, ρ_k^t is the mean square error (MSE) weight for UE k at slot t, and e_k^t is the corresponding MSE. With an initial $\mathbf{w}_k^t$, we have $\rho_k^t = e_k^{t^{-1}}$, where $e_k^t = \mathbb{E}[(u_k^t y_k^t - x_k^t)^2] = u_k^{t^H} (\sum_{j \in \mathcal{K}} \mathbf{h}_k^{t^H} \mathbf{w}_j^t \mathbf{w}_j^{t^H} \mathbf{h}_k^t + \sigma_k^2) u_k^t - 2\mathbf{Re}\{u_k^{t^H} \mathbf{h}_k^{t^H} \mathbf{w}_k^t\} + 1$ with $u_k^t = \frac{\mathbf{h}_k^{t^H} \mathbf{w}_k^t}{\sum_{j \in \mathcal{K}} \mathbf{h}_k^{t^H} \mathbf{w}_j^t \mathbf{w}_j^{t^H} \mathbf{h}_k^t + \sigma_k^2}$ being the optimal receiver.

By proper rearrangement, the SINR constraints in (3) can be rewritten as a convex second-order cone (SOC) constraint [10], that is,

$$\sqrt{\sum_{j \neq k} |\mathbf{h}_k^{t^H} \mathbf{w}_j^t|^2 + \sigma_k^2} \leq \frac{1}{\sqrt{\gamma_k}} \mathrm{Re}\{\mathbf{h}_k^{t^H} \mathbf{w}_k^t\}, \ \mathrm{Im}\{\mathbf{h}_k^{t^H} \mathbf{w}_k^t\} = 0. \tag{29}$$

With obtained ρ_k^t and u_k^t, the beamforming vector $\mathbf{w}_k^t$ can be attained solving [36]

$$\min_{\mathbf{w}_k^t} \sum_k \mathbf{w}_k^{tH} (\sum_{j \in \mathcal{K}} \eta Q_{u,j}^t \rho_j^t u_j^{t^H} \mathbf{h}_j^t \mathbf{h}_j^{t^H} u_j^t - \sum_i \eta q_i^t \mathbf{B}_i) \mathbf{w}_k^t - 2 \sum_k \eta Q_{u,k}^t \rho_k^t \mathbf{Re}\{u_k^{t^H} \mathbf{h}_k^{t^H} \mathbf{w}_k^t\}, \tag{30}$$

which is a quadratic program with the convex SOC constraint (29), and can also be solved using off-the-shelf convex solvers. Problem (25d) can then be solved by iterating between $\mathbf{w}_k^t$, u_k^t and ρ_k^t until $\mathbf{w}_k^t$ converges.

The proposed OER strategy is summarized in **Algorithm 1**.

Algorithm 1 Proposed OER Algorithm

1: Initialize the virtual queue lengths q_i^0, q_e^0 and stepsize η.
2: **for** $t = 1, 2, \ldots$ **do**
3: The APs deliver their transmission queue information $Q_{u,k}^t$ of UE k to VM k.
4: Each VM processes data with the optimal service rate in (27), and each AP transmits data to UEs with the optimal beamforming vector by solving (30).
5: The CPU and APs perform two-way energy transactions with the grid based on the optimal P_e^t and P_i^t, and charge or discharge the batteries based on the optimal $P_{b,e}^t$ and $P_{b,i}^t$, by solving (25a) and (25b).
6: Update the queue $\boldsymbol{Q}^{t+1} = \{Q_{e,k}^{t+1}, Q_{u,k}^{t+1}, q_i^{t+1}, q_e^{t+1}\}$ via the dynamics (5) and (24).
7: **end for**

B. PV Panel/Battery Sizing

We proceed to minimize the total system cost in (17) by selecting the sizes of the PV panels and batteries for each AP. Note that the PV panel/battery sizing is one-off and done before the online resource allocation and energy trading, and can be achieved in light of the asymptotic optimality of Algorithm 1. Consider that the sizes are discrete and can be selected from a finite set, and the asymptotically optimal OPEX (i.e, the upper bound of the offline optimum F^*) can be obtained solving **S1** under each different combination of the PV panel and battery sizes. With the asymptotically optimal policy at hand and historical data, Monte Carlo methods can be utilized to optimize the panel and battery sizes before deployment. In this case, the PSO can be utilized to test different possible combinations of panel and battery sizes, and evaluate the overall system cost. The PSO-based PV panel/battery sizing algorithm can speed up the sizing procedure, compared to an exhaustive search [14], and is described as follows.

At each search iteration n, the position of the p-th particle is $\boldsymbol{X}_p^n = [\boldsymbol{X}_{p,1}^n, \ldots, \boldsymbol{X}_{p,I}^n]_{1 \times I}$, where $\boldsymbol{X}_{p,i}^n = \{S_i, C_i^{\max}\}$, $p = 1, \ldots, P$, with P being the total number of particles. The search velocity $\boldsymbol{V}_p^n$ and position $\boldsymbol{X}_p^n$ of the p-th particle are updated as follows:

$$\begin{aligned} \boldsymbol{V}_p^{n+1} = & w \cdot \boldsymbol{V}_p^n + c_1 \cdot rand_1 \cdot (Pbest_p^n - \boldsymbol{X}_p^n) \\ & + c_2 \cdot rand_2 \cdot (Gbest^n - \boldsymbol{X}_p^n), \end{aligned} \tag{31}$$

$$\boldsymbol{X}_p^{n+1} = \boldsymbol{X}_p^n + \boldsymbol{V}_p^{n+1}, \tag{32}$$

where w is the inertia weight; c_1 and c_2 are constant weights; $rand_1$ and $rand_2$ are random values from $[0, 1]$; $Pbest_p^n$ is the best position (i.e., the 2-tuple $\{S_i, C_i^{\max}\}$ minimizing the system cost in (17)) of particle p recorded by iteration n; $Gbest^n$ is the best position among all particles by iteration n.

Let N denote the total number of iterations. The optimal $\{S_i, C_i^{\max}\}$ can be obtained when the iteration number reaches N. Then, we carry out online resource allocation and energy trading running Algorithm 1. The joint PBS-OER strategy is presented in **Algorithm 2**.

Computational Complexity. The computational complexity of the proposed OER algorithm is $\mathcal{O}(\Lambda)$, where $\Lambda := L\left[I^{3.5} + (MIK)^{3.5} + K\right]$. Here, L indicates the required number of iterations till convergence in Steps 2-7 of Algorithm 1. As per each iteration, the complexities of solving problem (25a), (25b) and (25d) are $\mathcal{O}(I^{3.5})$, $\mathcal{O}(1^{3.5})$ and $\mathcal{O}((MIK)^{3.5})$ using the interior-point method, respectively. Computing the optimal VM processing rates via (27) incurs a complexity of $\mathcal{O}(K)$. The total complexity of the PBS-OER algorithm is $\mathcal{O}(PN\Lambda)$. The complexity of solving Problem **S1**

Algorithm 2 Proposed PBS-OER Algorithm

1: Initialize particle positions $\boldsymbol{X}_p^0$ with random search velocities $\boldsymbol{V}_p^0$ for all particles.
2: **for** $n = 0, 1, 2, \ldots, N$ **do**
3: For each particle p, solve Problem **S1** with historical system parameters to calculate the minimum OPEX F^*, and sequentially the total cost in (17). Determine the corresponding $Pbest_p^n$ and $Gbest^n$.
4: Update the position $\boldsymbol{X}_p^{n+1}$ and velocity $\boldsymbol{V}_p^{n+1}$ of each particle via (31) and (32).
5: **end for**
6: Obtain the optimal $\{S_i, C_i^{\max}\}$ for all APs from the global best position $Gbest^n$.
7: Run Algorithm 1 to perform online resource allocation and energy trading.

in Step 3 of Algorithm 2 is $\mathcal{O}(\Lambda)$ for each iteration. The total number of iterations required is PN via the PSO approach. Compared to an exhaustive search-based approach with a complexity of $\mathcal{O}(S^I C^I \Lambda)$, PBS-OER significantly shortens the execution time. Here, S and C represent the number of candidate PV panels and battery sizes, respectively.

VI. Performance Guarantee

This section establishes the conditions under which the feasibility and (asymptotic) optimality of OER is guaranteed.

1) Queue Stability: By leveraging Lyapunov optimization [32], the queue stability under the OER is established:

Lemma 1 (Queue Stability): Suppose that there is a stationary policy $\mathcal{X}$: $\mathbb{E}[\sum_k (A_k^t - \mu_k^t)] \leq -\zeta$, $\mathbb{E}[\sum_k (\mu_k^t - r_k^t)] \leq -\zeta$, $\mathbb{E}[\sum_i (P_i^t - P_{c,i} - \sum_k \mathbf{w}_k^{t\,H} \mathbf{B}_i \mathbf{w}_k^t)] \leq -\zeta$, and $\mathbb{E}[P_e^t - k_c \sum_k (\mu_k^t)^3] \leq -\zeta$, where $\zeta > 0$ is a slack vector constant. Then, the OER algorithm guarantees the time-average queue length is bounded and grows linearly with $\frac{1}{\eta}$, i.e.,

$$\lim_{T\to\infty} \frac{1}{T} \sum_{t=0}^{T-1} \mathbb{E}[\sum_i (q_i^t) + q_e^t + \sum_k (Q_{e,k}^t + Q_{u,k}^t)] = \mathcal{O}(\frac{1}{\eta}).$$

Proof: Please refer to Appendix A. ∎

2) Feasibility Guarantee: The OER algorithm is designed to solve the relaxed Problem **S1.1**, where the instantaneous battery capacity constraint in (15c) is replaced by the long-term stability requirement. Nevertheless, we can prove that the derived policy is feasible for the original **S1**, i.e., satisfying (15c), by appropriately initializing η and $\{q_i^0, q_e^0, \forall i\}$.

Theorem 1 (Feasibility): If the stepsize $\eta \geq \underline{\eta} := \frac{\overline{\alpha} - \underline{\beta}}{\min\{C_i^{\max} - C_i^{\min} + P_{b,i}^{\min} - P_{b,i}^{\max}, C_e^{\max} - C_e^{\min} + P_{b,e}^{\min} - P_{b,e}^{\max}\}}$ and the initial lengths of the virtual queues are $q_i^0 = C_i^0 - \frac{\overline{\alpha}}{\eta} - C_i^{\min} + P_{b,i}^{\min}$ and $q_2^0 = C_e^0 - \frac{\overline{\alpha}}{\eta} - C_e^{\min} + P_{b,e}^{\min}$, then it holds that $C_i^t \in [C_i^{\min}, C_i^{\max}]$ and $C_e^t \in [C_e^{\min}, C_e^{\max}]$ under the OER algorithm, and the algorithm is feasible.

Proof: Please refer to Appendix B. ∎

Theorem 1 affirms that the OER is feasible for both the relaxed problem **S1.1** and the original **S1**, if the stepsize and the initial lengths of the virtual queues are properly configured.

3) Asymptotic Optimality: Finally, we can establish:

Theorem 2 (Asymptotic Optimality): With the stepsize and the initial virtual queues specified in Theorem 1, the OER yields asymptotic optimality and feasibility for **S1.1**, i.e.,

$$F^* \leq \lim_{T\to\infty} \frac{1}{T} \sum_{t=0}^{T-1} \mathbb{E}[\sum_i G_R(P_i^t) + G_B(P_e^t)] \leq F^* + \eta B,$$

where the constant $B := \frac{1}{2}[(\max\{P_{b,i}^{\max}, -P_{b,i}^{\min}\})^2 + (\max\{P_{b,e}^{\max}, -P_{b,e}^{\min}\})^2 + (A^{\max})^2 + 2(\mu^{\max})^2 + (r^{\max})^2]$, $A^{\max} = \max_k A_k^t$, $\mu^{\max} = \max_k \mu_k^t$, and $r^{\max} = \max_k r_k^t$.

Proof: Please refer to Appendix C. ∎

Theorem 2 indicates that the average cost of Problem **S1.1** under the OER converges to an $\mathcal{O}(\eta)$ close-to-optimal solution. The gap to the optimal (offline) solution diminishes as $\eta \to 0$. Based on Lemma 1, a cost-queue tradeoff of $[\eta, 1/\eta]$ is revealed. With $\eta = \underline{\eta}$, the optimality loss of the OER is $\underline{\eta} B = \frac{(\overline{\alpha} - \underline{\beta}) B}{\min\{C_i^{\max} - C_i^{\min} + P_{b,i}^{\min} - P_{b,i}^{\max}, C_e^{\max} - C_e^{\min} + P_{b,e}^{\min} - P_{b,e}^{\max}\}}$. The optimality loss is small, when $(\overline{\alpha} - \underline{\beta})$ is small or the battery capacities $C_i^{\max}$ and $C_e^{\max}$ are large. The proposed OER can approach the optimal F^* by properly choosing η.

VII. Simulation Results

In this section, extensive numerical tests are carried out to verify the proposed PBS-OER algorithm and validate the analyses presented in Section V.

A. Experiment Setup

We consider a green CF-RAN, where there are $I = 4$ APs, each with $M = 2$ transmit antennas, and $K = 20$ UEs. We use a custom-built numerical simulation platform developed in MATLAB. This platform rigorously implements the system models described in Section II (including the double-layer queueing dynamics, battery state-of-charge evolution, and wireless channel fading) and solves the decomposed subproblems using either closed-form solutions or convex optimization, i.e., standard interior-point method. For the wireless channel, we adopt a composite fading model that combines large-scale path loss with small-scale Rayleigh fading, where the path loss exponent is set to 3.5 and the Rayleigh distribution has unit variance. The fronthaul capacity $C_{\text{fh},i}$ is set to 1 Gbps. The task arrival process A_k^t is modeled as a scaled representation of real-world application traffic obtained from the OpenAirInterface (OAI) platform [37], with an average rate of 4 Mnats. Renewable energy variability is captured using real solar insolation data collected at the SolarTech Lab, Politecnico di Milano, Italy [38]. The size of the PV panels is picked from $[1, 2, \ldots, 7]$ m^2, and the battery capacity is picked from $[30, 40, \ldots, 90]$ kW [14]. The energy buying price α^t yields a folded normal distribution, i.e., $\alpha^t = |x|$ with $x \sim \mathcal{N}(3, 3)$, while the selling price is set to $\beta^t = r\alpha^t$ with $r = 0.5$ [31]. The stepsize is set to $\eta = \underline{\eta}$ (cf. **Theorem 1**). The default system parameters are listed in Table III.

The following alternatives are compared to PBS-OER to evaluate the benefit of two-way energy trading, RES and long-term planning.

TABLE III
SIMULATION PARAMETERS [31]

	Parameter	Value	Parameter	Value	Parameter	Value	Parameter	Value	Parameter	Value	Parameter	Value
System	γ_k	0.1	$\eta_{\text{ch}}, \eta_{\text{dis}}$	0.95	k_{c}	10^{-16}	C_{pv}	100 \$/m^2	C_{bat}	40 \$/kW	$P_{c,i}$	1 kW
AP i	$P_{g,i}^{\min}$	0	$P_{g,i}^{\max}$	50 kW	$C_i^{\min}$	5 kW	C_i^0	5 kW	$P_{b,i}^{\min}$	-10 kW	$P_{b,i}^{\max}$	10 kW
CPU	P_{coord}	100 W	$\mu_k^{\max}$	10 Mbps	$C_e^{\min}$	5 kW	C_e^0	5 kW	$P_{b,e}^{\min}$	-10 kW	$P_{b,e}^{\max}$	10 kW

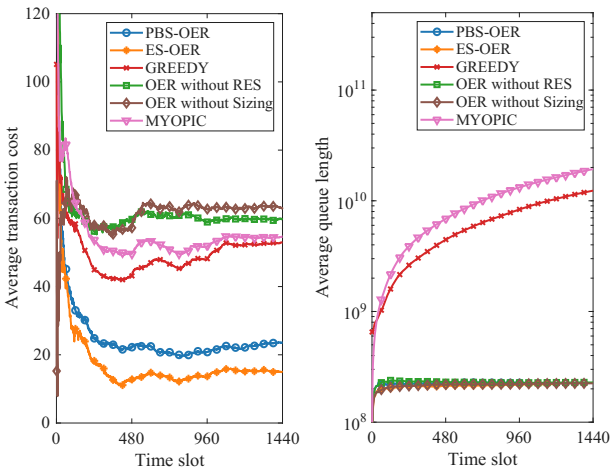

Fig. 2. Average system cost (i.e., long-term OPEX and CAPEX) and time-average queue length ($\eta = \underline{\eta}$).

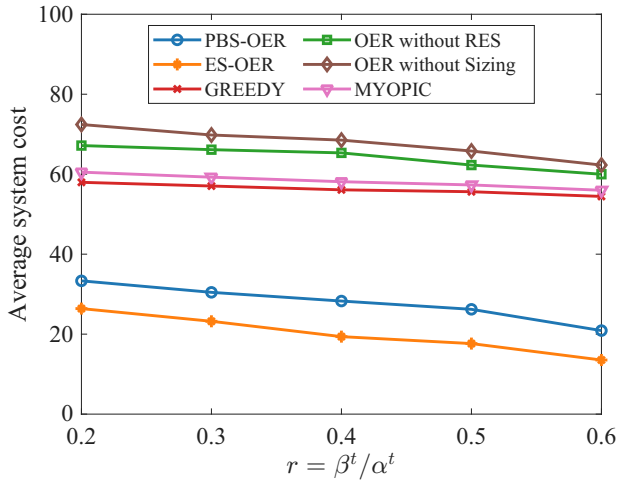

Fig. 3. Average system cost versus $r = \beta^t/\alpha^t$ ($\eta = \underline{\eta}$).

1) Joint Exhaustive Search-based Sizing and OER (ES-OER): This algorithm solves the sizing problem (17) using exhaustive search over all possible size combinations of PV panel and battery, and provides a lower bound of system cost.

2) Greedy Algorithm: In this algorithm, instantaneous decisions $\{\mathbf{w}_k^t, \mu_k^t, P_i^t, P_e^t\}$ are directly derived per slot by solving (16) with convex solvers. Any surplus or shortfall energy must be traded per slot to minimize the instantaneous cost.

3) OER without RES: It follows the proposed OER algorithm to optimize the time-average system cost. However, this algorithm does not utilize renewable energy. It only uses energy purchased from the grid, as opposed to OER.

4) OER without (PV panel and battery) Sizing: This algorithm randomly selects the sizes of PV panels and batteries from the candidate sets. The resource allocation is conducted online in the same way as described in Algorithm 1.

5) Myopic Algorithm [19]: This algorithm follows the proposed sizing scheme. It performs resource allocation myopically to minimize the instantaneous cost slot-by-slot without energy selling.

B. Performance Evaluation

Fig. 2(a) compares the average system costs of the considered algorithms. It is seen that PBS-OER converges to the lower bound (i.e., ES-OER), while Greedy, OER without RES, OER without Sizing and Myopic incur about 55.51%, 60.5%, 62.7%, and 56.9% higher costs, respectively. This is because PBS-OER takes advantage of the PV panel/battery sizing, RES, fluctuating energy prices, and the battery to store low-price energy for future use. In contrast, the Greedy algorithm trades any abundance or shortage of energy at the current slot to reduce the instantaneous cost. Similarly, Myopic follows a Greedy-like trend but with higher costs, as it does not sell energy and wastes surplus renewables. In Fig. 2(b), the average queue lengths of the OER-based algorithms achieve similar convergent values, while those of Greedy and Myopic keep rising, as these shortsighted algorithms minimize instantaneous costs while overlooking queue dynamics. With a convergent queue length, the system stability is ensured by the proposed OER, as stated in Lemma 1.

Fig. 3 shows the average system cost versus the price ratio $r = \beta^t/\alpha^t$ with fixed α^t. Clearly, the average costs of the considered algorithms decrease as r grows, since the system can make more profits with a higher β^t. The OER-based algorithms, i.e., PBS-OER, ES-OER, OER without RES, and OER without Sizing, can benefit more since the optimality gap $\underline{\eta}B$ narrows as r grows (or $(\overline{\alpha} - \underline{\beta})$ in $\underline{\eta}$ diminishes).

Fig. 4 plots the average system cost and running time of different algorithms versus the number of UEs K. In Fig. 4(a), it is clear that the average system costs increase with UEs, since the communication load is increasingly heavier. The costs of Greedy and Myopic, however, remain unchanged under different number of UEs at the cost of increasing queue lengths. Although ES-OER achieves the lowest average system cost, it undergoes a prohibitive computational complexity as validated in Fig. 4(b), when the number of UEs is large.

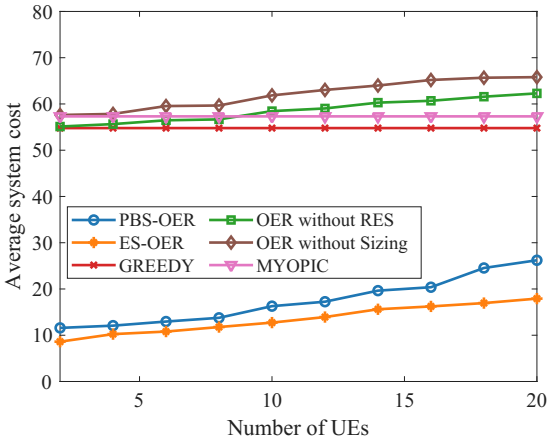

(a)

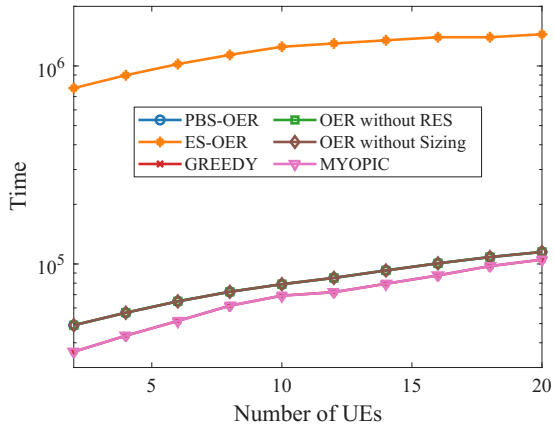

(b)

Fig. 4. Comparison of the average system cost and optimization time of different algorithms ($\eta = \underline{\eta}$).

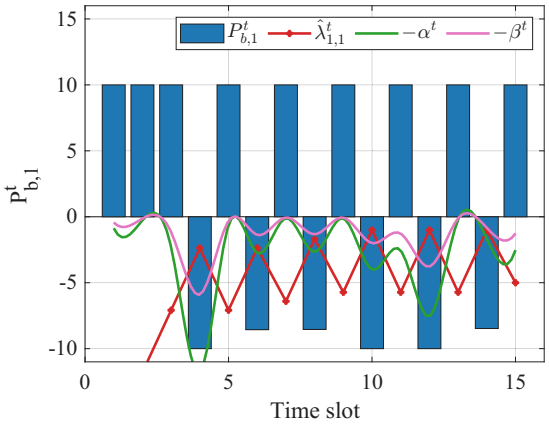

(a) Power schedule of AP_1

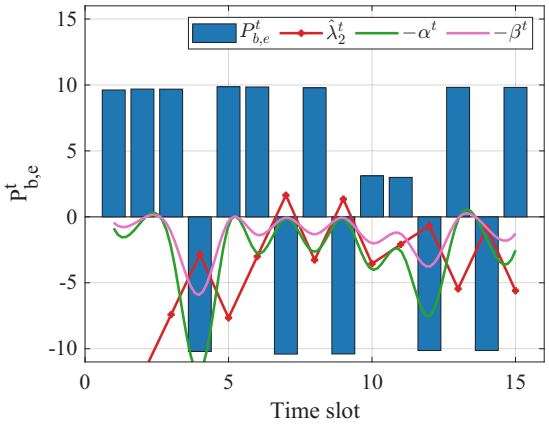

(b) Power schedule of the CPU

Fig. 5. Battery (dis)charging actions at AP_1 and the CPU ($C_1^{\max} = C_e^{\max} = 70$ kW, $\eta = \underline{\eta}$).

C. Analysis Verification

We demonstrate the asymptotic optimality and feasibility of OER with preserved system stability. First, we plot the energy prices α^t and β^t, the Lagrangian multipliers $\hat{\lambda}_{1,1}^t = \eta q_1^t$ and $\hat{\lambda}_2^t = \eta q_e^t$, and the battery (dis)charging amounts $P_{b,1}^t$ and $P_{b,e}^t$ in Fig. 5. It is observed from Fig. 5(a) that OER performs full battery charges $P_{b,1}^t = P_{b,1}^{\max}$ for AP_1 when $\hat{\lambda}_{1,1}^t < -\alpha^t$ at $t = 1, 2, 3, 5, 7, 9, 11, 13, 15$; while full discharges $P_{b,1}^t = P_{b,1}^{\min}$ occur when $\hat{\lambda}_{1,1}^t > -\beta^t$ at $t = 4, 10, 12$. This concurs with the finding in Lemma 3 in Appendix B. The same battery (dis)charging rules are observed at the CPU from Fig. 5(b).

Fig. 6 validates the feasibility condition derived in **Theorem 1**; i.e., the SoCs of AP_1 and CPU are always feasible ($C_1^{\min} \leq C_1^t \leq C_1^{\max}$, $C_e^{\min} \leq C_e^t \leq C_e^{\max}$) when $\eta = \underline{\eta}$. In contrast, if $\eta = 0.5\underline{\eta}$, the SoCs C_1^t and C_e^t exceed the battery capacity. The proposed OER obtained for the relaxed problem **S1.1** is feasible for the original problem **S1** after properly initializing η.

VIII. Concluding Remarks

In this paper, PV panel/battery sizing and resource allocation were investigated for renewable energy-powered CF-RAN. Leveraging PSO and the stochastic subgradient descent techniques, an offline sizing and online resource allocation and energy trading strategy was developed to minimize the total system cost. Applying the Lyapunov optimization technique, we proved that our PBS-OER algorithm is a feasible and asymptotically optimal strategy for the OPEX minimization problem, even without knowing the information of system dynamics *a-priori*. Simulations indicated that PBS-OER saves the average system cost by 62.7%, compared to its alternatives.

Appendix

A. Proof of Lemma 1

By generalizing the Lyapunov optimization, we start this proof with the following lemma.

Lemma 2: If $\boldsymbol{\xi}^t := \{I_i^t, E_e^t, A_k^t, \mathbf{h}_k^t, \alpha^t, \beta^t\}$ is i.i.d., there exists a stationary control strategy P^{stat}, which satisfies (5), (8), (11), (29) and guarantees: $\mathbb{E}[F^{stat}(X^t)] = \widetilde{F}^*$, $\mathbb{E}[\sum_k (A_k^t - \mu_k^{t,stat})] \leq -\zeta$, $\mathbb{E}[\sum_k (\mu_k^{t,stat} - r_k^t)] \leq -\zeta$, $\mathbb{E}[\sum_i (P_i^{t,stat} - P_{c,i} - \sum_k \mathbf{w}_k^{t,stat^H} \mathbf{B}_i \mathbf{w}_k^{t,stat}] \leq -\zeta$, and $\mathbb{E}[P_e^{t,stat} - k_c \sum_k (\mu_k^{t,stat})^3] \leq -\zeta$, where $F^{stat}(X^t)$ is the system cost under P^{stat}, $\{\mathbf{w}_k^{t,stat}, \mu_k^{t,stat}, P_i^{t,stat}, P_e^{t,stat}, \forall i, k, t\}$ are the variables.

Proof: This follows [32] and is suppressed for brevity. ■

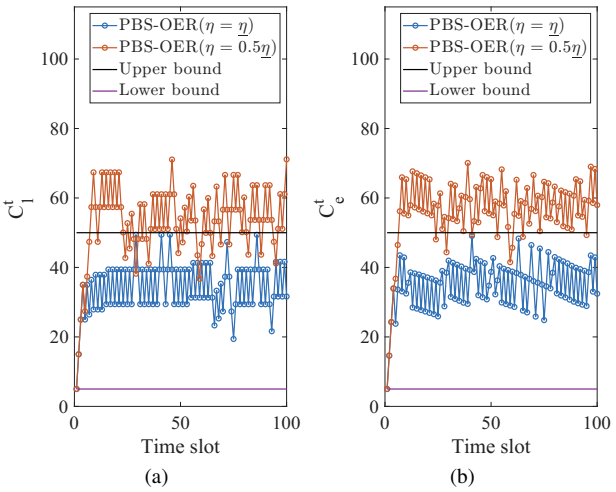

Fig. 6. Battery SoC at AP_1 and the CPU under the proposed PBS-OER ($C_1^{\max} = C_e^{\max} = 50$ kW, $\eta = \underline{\eta}$).

Lemma 2 shows that the stationary P^{stat} leads to the optimal cost of Problem **S1.1**, and the expected cost per t equals the optimal time-average cost. Based on the queue evolutions in (5), we have [32]

$$\begin{aligned}(Q_{e,k}^{t+1})^2 &= ([Q_{e,k}^t - \mu_k^t]^+ + A_k^t)^2 \\ &\le (Q_{e,k}^t)^2 + 2Q_{e,k}^t(A_k^t - \mu_k^t) + \underbrace{(A^{\max})^2 + (\mu^{\max})^2}_{2B_1},\end{aligned} \tag{33}$$

where $A^{\max} = \max_k A_k^t$, and $\mu^{\max} = \max_k \mu_k^t$.

Similarly, with $r^{\max} = \max_k r_k^t$, we have

$$\begin{aligned}(Q_{u,k}^{t+1})^2 &= ([Q_{u,k}^t - r_k^t]^+ + \mu_k^t)^2 \\ &\le (Q_{u,k}^t)^2 + 2Q_{u,k}^t(\mu_k^t - r_k^t) + \underbrace{(\mu^{\max})^2 + (r^{\max})^2}_{2B_2},\end{aligned} \tag{34}$$

From (11) and (24), it readily follows that

$$\begin{aligned}(q_i^{t+1})^2 &= (q_i^t + P_i^t - P_{c,i} - \sum_k \mathbf{w}_k^{tH}\mathbf{B}_i\mathbf{w}_k^t)^2 \\ &\le (q_i^t)^2 + 2q_i^t(P_i^t - P_{c,i} - \sum_k \mathbf{w}_k^{tH}\mathbf{B}_i\mathbf{w}_k^t) + \underbrace{(\max\{P_{b,i}^{\max}, -P_{b,i}^{\min}\})^2}_{2B_3}; \\ (q_e^{t+1})^2 &= (q_e^t + P_e^t - k_{\text{c}}\sum_k (\mu_k^t)^3)^2 \\ &\le (q_e^t)^2 + 2q_e^t(P_e^t - k_{\text{c}}\sum_k (\mu_k^t)^3) + \underbrace{(\max\{P_{b,e}^{\max}, -P_{b,e}^{\min}\})^2}_{2B_4}.\end{aligned} \tag{35}$$

Let $V(t) := \frac{1}{2}[\sum_i (q_i^t)^2 + (q_e^t)^2 + \sum_k (Q_{e,k}^t)^2 + \sum_k (Q_{u,k}^t)^2]$ denote the Lyapunov function. According to (33)-(35), the Lyapunov drift can be written as

$$\begin{aligned}\Delta V(t) := V(t+1) - V(t) &\le \sum_i q_i^t(P_i^t - P_{c,i} - \sum_k \mathbf{w}_k^{tH}\mathbf{B}_i\mathbf{w}_k^t) + \\ q_e^t(P_e^t - k_{\text{c}}\sum_k (\mu_k^t)^3) &+ \sum_k Q_{e,k}^t(A_k^t - \mu_k^t) + \sum_k Q_{u,k}^t(\mu_k^t - r_k^t) + B.\end{aligned}$$

where $B = B_1 + B_2 + B_3 + B_4$. Taking expectations and adding $\frac{1}{\eta}\mathbb{E}[\sum_i G_R(P_i^t) + G_B(P_e^t)]$ on both sides, it follows that

$$\begin{aligned}&\mathbb{E}[\Delta V(t)] + \frac{1}{\eta}\mathbb{E}[\sum_i G_R(P_i^t) + G_B(P_e^t)] \\ &\le B + \frac{1}{\eta}\mathbb{E}\Big\{[\sum_i G_R(P_i^t) + G_B(P_e^t)] + \eta q_e^t(P_e^t - k_{\text{c}}\sum_k (\mu_k^t)^3) \\ &\quad + \eta\sum_i q_i^t(P_i^t - P_{c,i} - \sum_k \mathbf{w}_k^{tH}\mathbf{B}_i\mathbf{w}_k^t) \\ &\quad + \eta\sum_k Q_{e,k}^t(A_k^t - \mu_k^t) + \eta\sum_k Q_{u,k}^t(\mu_k^t - r_k^t)\Big\} \\ &\le B + \frac{1}{\eta}\mathbb{E}\Big\{F^{stat}(X^t) + \eta q_e^t(P_e^{t,stat} - k_{\text{c}}\sum_k (\mu_k^{t,stat})^3) \\ &\quad + \eta\sum_i q_i^t(P_i^{t,stat} - P_{c,i} - \sum_k \mathbf{w}_k^{t,stat^H}\mathbf{B}_i\mathbf{w}_k^{t,stat}) \\ &\quad + \eta\sum_k Q_{e,k}^t(A_k^t - \mu_k^{t,stat}) + \eta\sum_k Q_{u,k}^t(\mu_k^{t,stat} - r_k^t)\Big\} \\ &\le B + \frac{1}{\eta}F^* - \zeta\mathbb{E}[\sum_i q_i^t + q_e^t + \sum_k (Q_{e,k}^t + Q_{u,k}^t)],\end{aligned} \tag{36}$$

where the second inequality holds since the OER minimizes L^t in (21) given all feasible strategies, such as P^{stat}. The last inequality is due to $\widetilde{F}^* \le F^*$ and Lemma 2.

Sum over t on both sides of (36). We have

$$\begin{aligned}&\sum_{t=0}^{T-1}\mathbb{E}[\Delta V(t)] + \frac{1}{\eta}\sum_{t=0}^{T-1}\mathbb{E}[\sum_i G_R(P_i^t) + G_B(P_e^t)] \\ &= \mathbb{E}[V(T)] - V(0) + \frac{1}{\eta}\sum_{t=0}^{T-1}\mathbb{E}[\sum_i G_R(P_i^t) + G_B(P_e^t)] \\ &\le T(B + \frac{1}{\eta}F^*) - \zeta\sum_{t=0}^{T-1}\mathbb{E}[\sum_i q_i^t + q_e^t + \sum_k (Q_{e,k}^t + Q_{u,k}^t)].\end{aligned}$$

Dividing both sides of (37) by T and then taking $T \to \infty$ yields Lemma 1.

B. Proof of Theorem 1

We start with the following lemma.

Lemma 3: The energy (dis)charged in the batteries under the proposed OER algorithm per slot, i.e., $P_{b,i}^t$ and $P_{b,e}^t$ satisfy

$$P_{b,i}^t(q_i^t) = \begin{cases} P_{b,i}^{\min}, \text{ if } q_i^t > \dfrac{-\underline{\beta}}{\eta}; \\ P_{b,i}^{\max}, \text{ if } q_i^t < \dfrac{-\overline{\alpha}}{\eta}; \end{cases} \quad P_{b,e}^t(q_e^t) = \begin{cases} P_{b,e}^{\min}, \text{ if } q_e^t > \dfrac{-\underline{\beta}}{\eta}; \\ P_{b,e}^{\max}, \text{ if } q_e^t < \dfrac{-\overline{\alpha}}{\eta}, \end{cases}$$

where $\overline{\alpha} := \max\{\alpha^t, \forall t\}$, and $\underline{\beta} := \min\{\beta^t, \forall t\}$.

Proof: According to $P_{b,i}^t = P_i^t - P_{c,i} - \sum_k \mathbf{w}_k^{tH}\mathbf{B}_i\mathbf{w}_k^t$, $P_{b,e}^t = P_e^t - k_{\text{c}}\sum_k (\mu_k^t)^3$, (25a) and (25b), we have

$$\begin{aligned}P_{b,i}^t(q_i^t) \in \arg\min_{P_{b,i}^t(q_i^t)} &\sum_i [G_R(P_{b,i}^t + P_{c,i} + \sum_k \mathbf{w}_k^{tH}\mathbf{B}_i\mathbf{w}_k^t) \\ &+ \eta q_i^t(P_{b,i}^t + \sum_k \mathbf{w}_k^{tH}\mathbf{B}_i\mathbf{w}_k^t)];\end{aligned}$$

$$\begin{aligned}P_{b,e}^t(q_e^t) \in \arg\min_{P_{b,e}^t(q_e^t)} &\sum_k [G_B(P_{b,e}^t + k_{\text{c}}\sum_k (\mu_k^t)^3) \\ &+ \eta q_e^t(P_{b,e}^t + k_{\text{c}}\sum_k (\mu_k^t)^3)],\end{aligned}$$

which lead to

i) If $P_{b,i}^t + P_{c,i} + \sum_k \mathbf{w}_k^{t^H}\mathbf{B}_i\mathbf{w}_k^t \geq E_i^t$ and $P_{b,e}^t + k_{\rm c}\sum_k(\mu_k^t)^3 \geq E_e^t$, then $G_R(P_{b,i}^t + P_{c,i} + \sum_k \mathbf{w}_k^{t^H}\mathbf{B}_i\mathbf{w}_k^t) = \alpha^t(P_{b,i}^t + P_{c,i} + \sum_k \mathbf{w}_k^{t^H}\mathbf{B}_i\mathbf{w}_k^t - E_i^t)$ and $G_B(P_{b,e}^t + k_{\rm c}\sum_k(\mu_k^t)^3) = \alpha^t(P_{b,e}^t + k_{\rm c}\sum_k(\mu_k^t)^3 - E_e^t)$. We must have

$$P_{b,i}^t(q_i^t)=\begin{cases} P_{b,i}^{\min}, \text{ if } \eta q_i^t+\alpha^t>0; \\ P_{b,i}^{\max}, \text{ if } \eta q_i^t+\alpha^t<0; \end{cases} P_{b,e}^t(q_e^t)=\begin{cases} P_{b,e}^{\min}, \text{ if } \eta q_e^t+\alpha^t>0; \\ P_{b,e}^{\max}, \text{ if } \eta q_e^t+\alpha^t<0. \end{cases}$$

ii) If $P_{b,i}^t + P_{c,i} + \sum_k \mathbf{w}_k^{t^H}\mathbf{B}_i\mathbf{w}_k^t < E_i^t$ and $P_{b,e}^t + k_{\rm c}\sum_k(\mu_k^t)^3 < E_e^t$, then $G_R(P_{b,i}^t + P_{c,i} + \sum_k \mathbf{w}_k^{t^H}\mathbf{B}_i\mathbf{w}_k^t) = \beta^t(P_{b,i}^t + P_{c,i} + \sum_k \mathbf{w}_k^{t^H}\mathbf{B}_i\mathbf{w}_k^t - E_i^t)$ and $G_B(P_{b,e}^t + k_{\rm c}\sum_k(\mu_k^t)^3) = \beta^t(P_{b,e}^t + k_{\rm c}\sum_k(\mu_k^t)^3 - E_e^t)$, we have

$$P_{b,i}^t(q_i^t)=\begin{cases} P_{b,i}^{\min}, \text{ if } \eta q_i^t+\beta^t>0; \\ P_{b,i}^{\max}, \text{ if } \eta q_i^t+\beta^t<0; \end{cases} P_{b,e}^t(q_e^t)=\begin{cases} P_{b,e}^{\min}, \text{ if } \eta q_e^t+\beta^t>0; \\ P_{b,e}^{\max}, \text{ if } \eta q_e^t+\beta^t<0. \end{cases}$$

Combining Cases i) and ii), we summarize that per slot t, if $\{\eta q_i^t, \eta q_e^t\} > \max\{-\alpha^t, -\beta^t\} = -\beta^t$, then $P_{b,i}^t(q_i^t) = P_{b,i}^{\min}$ and $P_{b,e}^t(q_e^t) = P_{b,e}^{\min}$; if $\{\eta q_i^t, \eta q_e^t\} < \min\{-\alpha^t, -\beta^t\} = -\alpha^t$, then $P_{b,i}^t(q_i^t) = P_{b,i}^{\max}$ and $P_{b,e}^t(q_e^t) = P_{b,e}^{\max}$. Lemma 3 is proved when the long-term horizon is considered. ∎

Lemma 3 indicates that a battery is fully discharged if its virtual energy queues are long enough (i.e., $q_i^t > \frac{-\underline{\beta}}{\eta}$ and $q_e^t > \frac{-\underline{\beta}}{\eta}$); and it is fully charged if the virtual energy queues are short (i.e., $q_i^t < \frac{-\overline{\alpha}}{\eta}$ and $q_e^t < \frac{-\overline{\alpha}}{\eta}$). Then, we first prove $\{q_i^t, \forall i, t\}$ is bounded by $[-\frac{\overline{\alpha}}{\eta} + P_{b,i}^{\min}, C_i^{\max} - C_i^{\min} - \frac{\overline{\alpha}}{\eta} + P_{b,i}^{\min}]$ using mathematic induction. Suppose q_i^0 and q_i^t are bounded by $[-\frac{\overline{\alpha}}{\eta} + P_{b,i}^{\min}, C_i^{\max} - C_i^{\min} - \frac{\overline{\alpha}}{\eta} + P_{b,i}^{\min}]$. We infer that q_i^{t+1} is also bounded as follows.

i) If $q_i^t \in (-\frac{\underline{\beta}}{\eta}, C_i^{\max} - C_i^{\min} - \frac{\overline{\alpha}}{\eta} + P_{b,i}^{\min}]$, it follows Lemma 3 that $q_i^{t+1} = q_i^t + P_{b,i}^{\min} \in (-\frac{\underline{\beta}}{\eta} + P_{b,i}^{\min}, C_i^{\max} - C_i^{\min} - \frac{\overline{\alpha}}{\eta} + 2P_{b,i}^{\min}] \subseteq (-\frac{\overline{\alpha}}{\eta} + P_{b,i}^{\min}, C_i^{\max} - C_i^{\min} - \frac{\overline{\alpha}}{\eta} + P_{b,i}^{\min}]$. The last step follows, as $-\frac{\overline{\alpha}}{\eta} < -\frac{\underline{\beta}}{\eta}$ and $P_{b,i}^{\min} < 0$.

ii) If $q_i^t \in [-\frac{\overline{\alpha}}{\eta}, -\frac{\underline{\beta}}{\eta}]$, then $q_i^{t+1} = q_i^t + P_{b,i}^t \in [-\frac{\overline{\alpha}}{\eta} + P_{b,i}^{\min}, -\frac{\underline{\beta}}{\eta} + P_{b,i}^{\max}] \subseteq [-\frac{\overline{\alpha}}{\eta} + P_{b,i}^{\min}, C_i^{\max} - C_i^{\min} - \frac{\overline{\alpha}}{\eta} + P_{b,i}^{\min}]$. The last step follows, as $\eta \geq \underline{\eta}$.

iii) If $q_i^t \in [-\frac{\overline{\alpha}}{\eta} + P_{b,i}^{\min}, -\frac{\overline{\alpha}}{\eta})$, it follows that $q_i^{t+1} = q_i^t + P_{b,i}^{\max} \in [-\frac{\overline{\alpha}}{\eta} + P_{b,i}^{\min} + P_{b,i}^{\max}, -\frac{\overline{\alpha}}{\eta} + P_{b,i}^{\max}) \subseteq (-\frac{\overline{\alpha}}{\eta} + P_{b,i}^{\min}, C_i^{\max} - C_i^{\min} - \frac{\overline{\alpha}}{\eta} + P_{b,i}^{\min})$. The last step is due to $P_{b,i}^{\max} > 0$, $-\frac{\overline{\alpha}}{\eta} < -\frac{\underline{\beta}}{\eta}$, and $\eta \geq \underline{\eta}$.

Since $C_i^t = q_i^t + \frac{\overline{\alpha}}{\eta} + C_i^{\min} - P_{b,i}^{\min}$, we can derive that $C_i^t \in [C_i^{\min}, C_i^{\max}]$ per slot t. The same finding also applies to C_e^t. Theorem 1 is proved.

C. Proof of Theorem 2

By referring to the proof of Lemma 1, it follows that

$$\begin{aligned}
&\mathbb{E}[\Delta V(t)] + \frac{1}{\eta}\mathbb{E}[\sum_i G_R(P_i^t) + G_B(P_e^t)] \\
&\leq B + \frac{1}{\eta}\mathbb{E}\Big\{[\sum_i G_R(P_i^t) + G_B(P_e^t)] \\
&+ \eta\sum_i q_i^t(P_i^t - P_{c,i} - \sum_k \mathbf{w}_k^{t^H}\mathbf{B}_i\mathbf{w}_k^t) + \eta q_e^t(P_e^t - k_{\rm c}\sum_k(\mu_k^t)^3) \\
&+ \eta\sum_k Q_{e,k}^t(A_k^t - \mu_k^t) + \eta\sum_k Q_{u,k}^t(\mu_k^t - r_k^t)\Big\} \\
&= B + \frac{1}{\eta}L(\mathcal{X}(\eta\boldsymbol{Q}^t), \eta\boldsymbol{Q}^t) = B + \frac{1}{\eta}D(\eta\boldsymbol{Q}^t) \leq B + \frac{1}{\eta}\widetilde{F}^*,
\end{aligned} \tag{37}$$

where $\mathcal{X}(\eta\boldsymbol{Q}^t)$ collects the decision variables in (23) with $\boldsymbol{\lambda} = \eta\boldsymbol{Q}^t$. $L(\mathcal{X}(\eta\boldsymbol{Q}^t), \eta\boldsymbol{Q}^t) = D(\eta\boldsymbol{Q}^t)$. The last inequality of (37) follows from the weak duality: $D(\boldsymbol{\lambda}) \leq \widetilde{F}^*$.

Finally, we sum both sides of (37) through t and get

$$\begin{aligned}
&\sum_{t=0}^{T-1}\mathbb{E}[\Delta V(t)] + \frac{1}{\eta}\sum_{t=0}^{T-1}\mathbb{E}[\sum_i G_R(P_i^t) + G_B(P_e^t)] \\
&= \mathbb{E}[V(T)] - V(0) + \frac{1}{\eta}\sum_{t=0}^{T-1}\mathbb{E}[\sum_i G_R(P_i^t) + G_B(P_e^t)] \\
&\leq T(B + \frac{1}{\eta}\widetilde{F}^*),
\end{aligned}$$

which results in $\frac{1}{T}\sum_{t=0}^{T-1}\mathbb{E}[\sum_i G_R(P_i^t) + G_B(P_e^t)] \leq \widetilde{F}^* + \eta(B + \frac{V(0)}{T}) \leq F^* + \eta(B + \frac{V(0)}{T})$. Theorem 2 is proved.

REFERENCES

[1] X. Chen, X. Zhang, W. Ni, X. Wang, S. Zhang, Y. Sun, and S. Xu, "PV panel/battery sizing and resource allocation for smart-grid powered C-RAN," in *Proc. IEEE SPAWC*. IEEE, 2023, pp. 591–595.

[2] Y. Guo, D. Wang, X. Xia, Z. Zhang, J. Li, P. Zhu, and X. You, "Stochastic geometry analysis of scalable cell-free RAN with dynamic association and deployment," *IEEE J. Sel. Top. Signal Process.*, vol. 19, no. 2, pp. 398–411, 2025.

[3] A. Papazafeiropoulos, H. Q. Ngo, P. Kourtessis, S. Chatzinotas, and J. M. Senior, "Towards optimal energy efficiency in cell-free massive MIMO systems," *IEEE Trans. on Green Commun. Netw.*, vol. 5, no. 2, pp. 816–831, 2021.

[4] Y. Cao, Z. Zhang, X. Xia, P. Xin, D. Liu, K. Zheng, M. Lou, J. Jin, Q. Wang, D. Wang, Y. Huang, X. You, and J. Wang, "Implementation of a cell-free RAN system with distributed cooperative transceivers under ORAN architecture," *IEEE J. Sel. Areas Commun.*, vol. 43, no. 3, pp. 765–779, 2025.

[5] T. Dragičević, P. Siano, and S. S. Prabaharan, "Future generation 5G wireless networks for smart grid: A comprehensive review," *Energies*, vol. 12, no. 11, p. 2140, 2019.

[6] X. Wang, T. Chen, X. Chen, X. Zhou, and G. B. Giannakis, "Dynamic resource allocation for smart-grid powered MIMO downlink transmissions," *IEEE J. Sel. Areas Commun.*, vol. 34, no. 12, pp. 3354–3365, 2016.

[7] S. Hu, X. Chen, W. Ni, X. Wang, and E. Hossain, "Modeling and analysis of energy harvesting and smart grid-powered wireless communication networks: A contemporary survey," *IEEE Trans. Green Commun. Netw.*, vol. 4, no. 2, pp. 461–496, 2020.

[8] L. Liu, Z. Zhang, H. Zhang, Y. Zhang, and Y. Xu, "Two-timescale dynamic resource management in smart-grid powered heterogeneous cellular networks," *IEEE Trans. Wireless Commun.*, vol. 23, no. 4, pp. 2681–2695, Apr. 2024.

[9] L. Qi, B. Wu, X. Chen, L. Zhou, W. Ni, and A. Jamalipour, "Joint optimization of internet of things and smart grid for energy generation, battery (dis)charging, and information delivery," *IEEE Internet Things J.*, vol. 11, no. 12, pp. 21 647–21 658, Jun. 2024.

[10] X. Wang, X. Chen, T. Chen, L. Huang, and G. B. Giannakis, "Two-scale stochastic control for integrated multipoint communication systems with renewables," *IEEE Trans. Smart Grid*, vol. 9, no. 3, pp. 1822–1834, May. 2018.

[11] X. Chen, H. Wen, W. Ni, S. Zhang, X. Wang, S. Xu, and Q. Pei, "Distributed online optimization of edge computing with mixed power supply of renewable energy and smart grid," *IEEE Trans. Commun.*, vol. 70, no. 1, pp. 389–403, 2022.

[12] X. Chen, S. Chen, W. Ni, X. Wang, S. Zhang, S. Zhang, Y. Sun, S. Xu, and A. Jamalipour, "Optimal two-timescale configuration of mobile edge computing with mixed energy supply," *IEEE Trans. Smart Grid*, vol. 15, no. 5, pp. 4765–4778, 2024.

[13] A. Israr, Q. Yang, W. Li, and A. Y. Zomaya, "Renewable energy powered sustainable 5G network infrastructure: Opportunities, challenges and perspectives," *J. Netw. Comput. Appl.*, vol. 175, p. 102910, 2021.

[14] M. Javidsharifi, H. Pourroshanfekr, T. Kerekes, D. Sera, S. Spataru, and J. M. Guerrero, "Optimum sizing of photovoltaic and energy storage systems for powering green base stations in cellular networks," *Energies*, vol. 14, no. 7, p. 1895, 2021.

[15] M. S. Hossain, K. Z. Islam, A. G. Alharbi, M. Shafiullah, M. R. Islam, and A. Fekih, "Optimal design of a hybrid solar PV/BG-powered heterogeneous network," *Sustainability*, vol. 14, no. 4, p. 2201, 2022.

[16] M. Mendil, A. De Domenico, V. Heiries, R. Caire, and N. Hadjsaid, "Battery-aware optimization of green small cells: Sizing and energy management," *IEEE Trans. Green Commun. Netw.*, vol. 2, no. 3, pp. 635–651, 2018.

[17] T. Pamuklu and C. Ersoy, "Reducing the total cost of ownership in radio access networks by using renewable energy resources," *Wireless Netw.*, vol. 26, pp. 1667–1684, 2020.

[18] Ö. T. Demir and E. Björnson, "Joint power control and LSFD for wireless-powered cell-free massive MIMO," *IEEE Trans. Wireless Commun.*, vol. 20, no. 3, pp. 1756–1769, 2020.

[19] F. Moradi, V. Hakami, and S. V. Azhari, "Resource allocation in cell-free massive MIMO networks with hybrid energy supplies," *IEEE Access*, 2023.

[20] Y. Zhang, Y. Jiang, Y. Huang, and F.-C. Zheng, "Energy consumption optimization in cell-free massive MIMO systems with hybrid energy supply," *IEEE Wireless Commun. Lett.*, vol. 14, no. 1, pp. 98–102, 2025.

[21] P. Zhu, "A resource allocation method for C-RAN systems that balances long-term energy efficiency and network stability," *CN 111107645 A*, December 2019.

[22] D. Zeng, J. Zhang, S. Guo, L. Gu, and K. Wang, "Take renewable energy into CRAN toward green wireless access networks," *IEEE Netw.*, vol. 31, no. 4, pp. 62–68, 2017.

[23] V. Chamola and B. Sikdar, "Outage estimation for solar powered cellular base stations," in *Proc. ICC*. IEEE, 2015, pp. 172–177.

[24] J. Tang, W. P. Tay, and T. Q. Quek, "Cross-layer resource allocation with elastic service scaling in cloud radio access network," *IEEE Trans. Wireless Commun.*, vol. 14, no. 9, pp. 5068–5081, 2015.

[25] L. Chen and N. Li, "On the interaction between load balancing and speed scaling," *IEEE J. Sel. Areas Commun.*, vol. 33, no. 12, pp. 2567–2578, 2015.

[26] J. Tang, W. P. Tay, and Y. Wen, "Dynamic request redirection and elastic service scaling in cloud-centric media networks," *IEEE Trans. Multimedia*, vol. 16, no. 5, pp. 1434–1445, 2014.

[27] G. Rami, T. Tran-Quoc, N. Hadjsaid, and J. Mertz, "Energy supply for remote base transceiver stations of telecommunication," in *Proc. IEEE PES GM*. IEEE, 2004, pp. 1916–1921.

[28] K. Girigoudar, M. Yao, J. L. Mathieu, and L. A. Roald, "Integration of centralized and distributed methods to mitigate voltage unbalance using solar inverters," *IEEE Trans. Smart Grid*, vol. 14, no. 3, pp. 2034–2046, 2023.

[29] J.-O. Lee and Y.-S. Kim, "Novel battery degradation cost formulation for optimal scheduling of battery energy storage systems," *Int. J. Electr. Power Energy Syst.*, vol. 137, p. 107795, 2022.

[30] A. Gailani, M. Al-Greer, M. Short, and T. Crosbie, "Degradation cost analysis of Li-Ion batteries in the capacity market with different degradation models," *Electronics*, vol. 9, no. 1, 2020.

[31] X. Wang, Y. Zhang, T. Chen, and G. B. Giannakis, "Dynamic energy management for smart-grid-powered coordinated multipoint systems," *IEEE J. Sel. Areas Commun.*, vol. 34, no. 5, pp. 1348–1359, 2016.

[32] Neely and J. Michael, "Stochastic network optimization with application to communication and queueing systems," *Synth. Lect. Commun. Netw.*, vol. 3, no. 1, p. 211, 2010.

[33] X. Chen, W. Ni, T. Chen, I. B. Collings, X. Wang, R. P. Liu, and G. B. Giannakis, "Multi-timescale online optimization of network function virtualization for service chaining," *IEEE Trans. Mobile Comput.*, vol. 18, no. 12, pp. 2899–2912, Dec. 2019.

[34] S. Boyd, S. P. Boyd, and L. Vandenberghe, *Convex optimization*. Cambridge university press, 2004.

[35] Q. Shi, M. Razaviyayn, Z.-Q. Luo, and C. He, "An iteratively weighted MMSE approach to distributed sum-utility maximization for a MIMO interfering broadcast channel," *IEEE Trans. Signal Process.*, vol. 59, no. 9, pp. 4331–4340, 2011.

[36] B. Dai and W. Yu, "Sparse beamforming and user-centric clustering for downlink cloud radio access network," *IEEE Access*, vol. 2, pp. 1326–1339, 2014.

[37] B. Romdhanne, N. Navid, R. Knopp, and B. Christian, "Openairinterface large-scale wireless emulation platform and methodology," *ACM*, 2011.

[38] S. Leva, A. Nespoli, S. Pretto, M. Mussetta, and E. Ogliari, "Photovoltaic power and weather parameters," 2020. [Online]. Available: https://dx.doi.org/10.21227/42v0-jz14

Xiaojing Chen (Member, IEEE) received the B.S. degree in communication science and engineering and the Ph.D. degree in electromagnetic field and microwave technology from Fudan University, China, in 2013 and 2018, respectively, and the Ph.D. degree in engineering from Macquarie University, Australia, in 2019. She is currently an associate professor with Shanghai University, China. Her research interests include wireless communications for AI, green wireless communications, and edge intelligence.

Yijun Ding received the B.E. degree from the School of Communication and Information Engineering, Shanghai University, Shanghai, China, in 2023. He is currently pursuing the master's degree with Shanghai University, Shanghai, China. His current research interests include green wireless communications and edge computing.

Xiaomei Zhang received the B.E. and M.S. degree from the School of Communication and Information Engineering, Shanghai University, Shanghai, China, in 2021 and 2024, respectively.

Wei Ni (Fellow, IEEE) received the B.E. and Ph.D. degrees in Electronic Engineering from Fudan University, Shanghai, China, in 2000 and 2005, respectively. He is the Associate Dean (Research) in the School of Engineering, Edith Cowan University, Perth, and a Conjoint Professor at the University of New South Wales, Sydney, Australia. He is also a Technical Expert at Standards Australia with focus on the international standardization of Big Data and AI. He was a Deputy Project Manager at the Bell Labs, Alcatel/Alcatel-Lucent from 2005 to 2008; a Senior Research Engineer at Nokia from 2008 to 2009; and a Senior Principal Research Scientist and Group Leader at the Commonwealth Scientific and Industrial Research Organisation (CSIRO) from 2009 to 2025. He has co-authored four books, eleven book chapters, over 550 technical papers, 27 patents, and ten standard proposals accepted by IEEE. His research interests include machine learning, online learning, stochastic optimization, and their applications to system efficiency, integrity, and resilience. He has been an Editor for IEEE Transactions on Wireless Communications since 2018, IEEE Transactions on Vehicular Technology since 2022, IEEE Transactions on Information Forensics and Security and IEEE Communication Surveys and Tutorials since 2024, and IEEE Transactions on Network Science and Engineering since 2025. He served as Secretary, Vice-Chair, and Chair of the IEEE VTS NSW Chapter from 2015 to 2022, Track Chair for VTC-Spring 2017, Track Co-chair for IEEE VTC-Spring 2016, Publication Chair for BodyNet 2015, and Student Travel Grant Chair for WPMC 2014.

Yichuang Sun (Life Senior Member, IEEE) received the B.Sc. and M.Sc. degrees in communications and electronics engineering from Dalian Maritime University, Dalian, China, in 1982 and 1985, respectively, and the Ph.D. degree in communications and electronics engineering from the University of York, York, U.K., in 1996. He is currently a Professor of communications and electronics, the Head of the Communications and Intelligent Systems Research Group, and the Head of the Electronic, Communication and Electrical Engineering Division with the School of Engineering and Computer Science, University of Hertfordshire, Hatfield, U.K. He has published over 420 articles and contributed ten chapters to edited books. He has also published four text and research books: Continuous-Time Active Filter Design (CRC Press, USA, 1999), Design of High Frequency Integrated Analog Filters (IEE Press, U.K., 2002), Wireless Communication Circuits and Systems (IET Press, 2004), and Test and Diagnosis of Analog, Mixed-Signal and RF Integrated Circuits—The Systems on Chip Approach (IET Press, 2008). His research interests are in the areas of wireless and mobile communications, RF and analog circuits, memristor circuits and systems, and machine learning and neuromorphic computing.

Xin Wang (Fellow, IEEE) received the B.Sc. and M.Sc. degrees in electrical engineering from Fudan University, Shanghai, China, in 1997 and 2000, respectively, and the Ph.D. degree in electrical engineering from Auburn University, Auburn, AL, USA, in 2004.

From September 2004 to August 2006, he was a Post-Doctoral Research Associate with the Department of Electrical and Computer Engineering, University of Minnesota, Minneapolis. In August 2006, he joined the Department of Electrical Engineering, Florida Atlantic University, Boca Raton, FL, USA, as an Assistant Professor, then he was promoted to a tenured Associate Professor in 2010. He is currently a Distinguished Professor and the Chair of the Department of Communication Science and Engineering, Fudan University. His research interests includes tochastic network optimization, energy-efficient communications, cross-layer design, and signal processing for communications. He is a member of the Signal Processing for Communications and Networking Technical Committee of IEEE Signal Processing Society and a Distinguished Speaker of the IEEE Vehicular Technology Society. He is a Senior Area Editor of the IEEE TRANSACTIONS ON SIGNAL PROCESSING and an Editor of the IEEE TRANSACTIONS ON WIRELESS COMMUNICATIONS and in the past served as an Associate Editor for the IEEE TRANSACTIONS ON SIGNAL PROCESSING, an Editor for the IEEE TRANSACTIONS ON VEHICULAR TECHNOLOGY, and an Associate Editor for the IEEE SIGNAL PROCESSING LETTERS.

Shunqing Zhang (Senior Member, IEEE) received the B.S. degree from the Department of Microelectronics, Fudan University, Shanghai, China, in 2005, and the Ph.D. degree from the Department of Electrical and Computer Engineering, Hong Kong University of Science and Technology, Hong Kong, in 2009. He was with the Communication Technologies Laboratory, Huawei Technologies from 2009 to 2014, and a Senior Research Scientist with Intel Labs from 2015 to 2017. Since 2017, he has been with the School of Communication and Information Engineering, Shanghai University, Shanghai, as a Full Professor. He has published more than 70 peer-reviewed journal and conference papers, and more than 50 granted patents. His current research interests include energy efficient 5G/5G+ communication networks, hybrid computing platform, and joint radio frequency and baseband design. He was the recipient of the Paper Award for Advances in Communications from IEEE Communications Society, in 2017.